DYNAMIC CHARACTERISTICS OF FILLED NATURAL RUBBER FOR EARTHQUAKE ENERGY APPLICATIONS

TEE YUN LU

FACULTY OF ENGINEERING
UNIVERSITY OF MALAYA
KUALA LUMPUR

2018

DYNAMIC CHARACTERISTICS OF FILLED NATURAL RUBBER FOR EARTHQUAKE ENERGY APPLICATIONS

TEE YUN LU

THESIS SUBMITTED IN FULFILMENT
OF THE REQUIREMENTS
FOR THE DEGREE OF MASTER OF ENGINEERING
SCIENCE

FACULTY OF ENGINEERING
UNIVERSITY OF MALAYA
KUALA LUMPUR

2018

UNIVERSITI MALAYA

ORIGINAL LITERARY WORK DECLARATION

Name of Candidate: Tee Yun Lu

Registration/Matrix No.:KGA130052

Name of Degree: Master of Engineering Science

Title of Project Paper/Research Report/Dissertation/Thesis ("this Work"): Dynamic Characteristics Of Filled Natural Rubber For Earthquake Energy Applications

Field of Study:Mechanical Aspect of Polymer

I do solemnly and sincerely declare that:

(1) I am the sole author/writer of this Work;
(2) This work is original;
(3) Any use of any work in which copyright exists was done by way of fair dealing and for permitted purposes and any excerpt or extract from, or reference to or reproduction of any copyright work has been disclosed expressly and sufficiently and the title of the Work and its authorship have been acknowledged in this Work;
(4) I do not have any actual knowledge nor do I ought reasonably to know that the making of this work constitutes an infringement of any copyright work;
(5) I hereby assign all and every rights in the copyright to this Work to the University of Malaya ("UM"), who henceforth shall be owner of the copyright in this Work and that any reproduction or use in any form or by any means whatsoever is prohibited without the written consent of UM having been first had and obtained;
(6) I am fully aware that if in the course of making this Work I have infringed any copyright whether intentionally or otherwise, I may be subject to legal action or any other action as may be determined by UM.

Candidate's Signature | Date

Subscribed and solemnly declared before,

Witness's Signature | Date

Name:
Designation:

DYNAMIC CHARACTERISTICS OF FILLED NATURAL RUBBER FOR EARTHQUAKE ENERGY APPLICATIONS

ABSTRACT

Apart from food and clothing, a secure shelter is a necessity for a civilised society. Buildings and structures are proves that a country is moving toward modernisation. During the service, high-rise buildings and architectural structures are prone to dynamic external forces such as earthquake and wind. Along this line, innovative means of enhancing structural functionality and safety against natural hazards such as active, hybrid and passive energy dissipation system have been carried out in recent years. Passive energy dissipation system is the preferable energy dissipation device due to its good performance, economic and easy maintenance. In this thesis, an original passive energy dissipation device in the form of sliding rubber damper (SRD) is proposed. The device is developed by utilizing the special characteristics of rubber as damper and metal plates as supporting material. In order to produce a device that is economic and durable, study on the dynamic characteristics of material is required. For this purpose, shear and combined tension-torsion fatigue tests on carbon black filled natural rubber are conducted. Two carbon black contents are considered: 10 wt% and 25 wt%. The fatigue test results are presented in the form of Wöhler curves where the maximum principal stretch and the strain energy density are used as fatigue predictors in combination with the concept of strain amplification factor to account for carbon black content. The modal analysis is subsequently carried out in order to investigate the vibration characteristics of the device. More precisely, the latter involves impact hammer testing and shaker testing on a structure model. Results showed that fatigue life of natural rubber with 25 wt% carbon black is longer than 10 wt%. Moreover, rubber with 25 wt% carbon black showed a better damping performance.

Keywords: fatigue lifetime, rubber, carbon black

CIRI-CIRI DINAMIK GETAH ASLI DIPENUHI KARBON HITAM UNTUK APLIKASI PELEPASAN TENAGA GEMPA BUMI

ABSTRAK

Selain daripada makanan dan pakaian, tempat tinggal yang selamat adalah satu keperluan bagi masyarakat yang bertamadun. Bangunan dan struktur yang membuktikan bahawa negara yang sedang bergerak ke arah pemodenan. Sepanjang perkhidmatan, bangunan-bangunan tinggi dan struktur seni bina terdedah kepada kuasa-kuasa luar yang dinamik seperti gempa bumi dan angin. Sehubungan ini, cara inovatif untuk meningkatkan fungsi struktur dan keselamatan terhadap bencana alam seperti aktif, hibrid dan pasif sistem pelesapan tenaga telah dijalankan pada tahun-tahun kebelakangan ini. Pelesapan tenaga pasif sistem adalah peranti pelesapan tenaga yang lebih baik disebabkan oleh prestasi yang baik, penyelenggaraan ekonomi dan mudah. Dalam tesis ini, peranti pelesapan tenaga pasif dalam bentuk gelongsor peredam getah (SRD) dicadangkan. Peranti ini dibangunkan dengan menggunakan ciri-ciri khas getah peredam dan logam plat sebagai bahan sokongan. Dalam usaha untuk menghasilkan peranti yang ekonomi dan tahan lama, kajian mengenai ciri-ciri dinamik bahan diperlukan. Untuk tujuan ini, ricih dan ujian gabungan kelesuan ketegangan-kilasan pada karbon hitam dipenuhi getah asli dijalankan. Kandungan dua karbon hitam digunakan: 10 wt% dan 25 wt%. Keputusan ujian kelesuan dibentangkan dalam bentuk keluk Wöhler di mana regangan prinsipal maksimum dan ketumpatan tenaga terikan digunakan sebagai peramal kelesuan. Analisis modal kemudiannya dijalankan untuk menyiasat ciri-ciri getaran peranti tersebut. Ujian getaran melibatkan ujian kesan tukul dan ujian shaker pada model struktur. Hasil kajian menunjukkan bahawa hayat lesu daripada getah asli dengan 25 wt% karbon hitam adalah lebih lama daripada 10 wt%. Selain itu, getah dengan 25 wt% karbon hitam menunjukkan prestasi redaman yang lebih baik.

Kata kunci: hayat kelesuan, getah, karbon hitam,

ACKNOWLEDGEMENTS

First and foremost, I would like to express my greatest gratitude to my supervisors Dr Andri Andriyana and Dr Meldi Suhatril for their patience in guiding me throughout the study. Their advice and motivations are the primary source for me to move forward till the end of my master study.

Next, I would also thank Prof Erwan Verron and Dr Bertrand Huneau from Ecole Centrale de Nantes, France for offering a research internship opportunity. This exchange program greatly widen my eyesight in both research and culture of France. The financial assistance from the Embassy of France is highly appreciated.

Apart from that, I would like to thank my friends in Faculty of Engineering. The supports and encouragement during the study is part of the memorable moments. The journey to success is full of joy and happiness with their companion.

My family for their endless encouragement when I made my decision to further study. Their supports and understanding energized me whenever I felt helpless. Thank you so much for everyone that stay by my side throughout these years.

TABLE OF CONTENTS

LIST OF FIGURES

LIST OF TABLES

LIST OF SYMBOLS AND ABBREVIATIONS

NR : Natural Rubber
SRD : Sliding rubber damper
IR : Isoprene rubber
ATH : Aluminium hydroxide
EG : Expandable graphine
EPDM : Ethylene propylene diene modified rubberr
SBR : Styrene butadiene rubber
BR : Polybutadiene rubber
IIR : Butyl rubber
NBR : Acrylonitrile-butadiene rubber
CR : Polychloroprene rubber
phr : Parts per hundreds
R : Maximum energy release rate
$^{\circ}C$: Degree celcius
λ_{loc} : Microscopic axial stretch
λ_{glo} : Macroscopic axial stretch
χ : Strain amplification factor
λ_{max} : Maximum principal stretch
$\hat{\eta}$: Viscocity suspension
$\eta_{\circ}$: Viscosity of incompressible fluid
ϕ : Volume fraction of spherical particles
$\hat{E}$: Elastic moduli of filled rubber
$E_{\circ}$: Elastic moduli of unfilled rubber
v_f : Filler volume fraction
$\hat{\varepsilon}$: Actual elongation
$\varepsilon_{\circ}$: Observed elongation
ASTM : American Society of Testing and Materials
wt% : Weight percentage
kN : Kilo Newton
mm : Millimeter
Hz : Hertz
t : Time
$\boldsymbol{e}_{1,2,3}$: Coordinate system
F : Deformation gradient tensor
B : Left Cauchy-Green tensor
u : Displacement
h : Thickness
$\lambda_{1,2,3}$: Principal stretch
W : Strain energy density
C : Left Cauchy-Green strain tensor
I : Identity tensor
τ : Twist per unit length
R : Radius
CB : Carbon black

CHAPTER 1: INTRODUCTION

1.1 Research background

Seismic vibration isolation devices is no longer an unknown term in the field of earthquake structural engineering community to reduce the earthquake-induced response on structural buildings. The application of these devices is widely utilised in most of the structures especially in the high earthquake risk countries. However it is worth to note that other than reducing the effect of earthquake, it is also useful in protecting the high-rise buildings from wind force.

Recent years, studies have been conducted to produce innovative structural control devices as a mean to protect buildings from either natural or human made hazards. There are various structural control systems available in the market to cope with different requirements of buildings. Passive, active, semi-active and hybrid type of control systems are available. Among these, the most popular is the passive system (Booth & Key, 2006).

In terms of effectiveness, passive system shows promising performance. One of the example is the base isolation system. The alternating layer of elastomeric and metal effectively absorb the seismic vibration from transmitting to the structure buildings. Being one of the most efficient isolator system, however, based isolation system needs to be installed during the construction of the building.

For the current building without the base isolator installed, the alternative would be the passive energy dissipation system, which can be installed on the structure after the building construction is done. Dampers, one of the passive energy dissipation system, could be an excellent solution for buildings which are not equipped with structural control systems. The commonly known dampers are viscous fluid dampers, viscoelastic dampers, yielding metallic dampers and friction dampers (Srinivas & Nakagawa, 2008). Even if Malaysia has never experienced major hazard from local earthquake, earthquake vibration from neighbouring countries could propagate to some parts of Malaysia. Thus, precaution actions on the effect of seismic vibration should be taken since most of high-rise buildings in Malaysia are not equipped with structural control system. Being a major world rubber producer, viscoelastic rubber dampers could be the best choice in Malaysia among the above mentioned dampers.

Classically, the performance of a structure when encounters earthquake vibration is assessed based on its ability to absorb and dissipate energy in a stable manner for a large number of cycles. In this case, the rubber energy dissipation devices are subjected to fluctuating loading which could lead to fatigue failure. Thus, the study on fatigue and vibration characteristics of rubber materials used for these applications becomes pre-requisite for durability and performance analysis.

1.2 Problem statement

Malaysia, surrounded by earthquake high risk zone which may be affected by the earthquake vibration from the neighboring countries. Structural control system is vital as a prevention to the potential hazard, yet not all infrastructure and high-rise building are well-equipped with the necessary protection system. The widely used passive structural control system is the most suitable from the aspect of technical aptitude and cost. Inspired by the effective use of rubber in automobile and aerospace industry for anti-vibration system, rubber is chosen as the main material in designing a new damper device for earthquake energy dissipation application. Prior to the actual application, study is needed to investigate the optimum rubber content used in this system including the fatigue lifetime and the vibration characteristic.

1.3 Objectives

The main objective of this thesis is to elucidate the fatigue characteristics of natural rubber with the consideration of the effect of carbon black. The optimum rubber material will be applied in the original proposed earthquake energy dissipation device.

In line with the main objective, the details are summarized as below:

1. To investigate the fatigue characteristics of natural rubber used for sliding rubber damper.

2. To investigate the effect of filler content on the fatigue life of natural rubber.

3. To investigate the effect of rubber damper on the vibration characteristic of structure and to propose a simple sliding rubber damper component as potential earthquake energy dissipation device in a structure.

1.4 Dissertation organization

This thesis is organized as follows. The content of the body started with Chapter 1, Introduction. This chapter includes the brief overview of the background, objectives and scopes of the work. This is followed by Chapter 2, Literature Review. Study of the past and current knowledge on this work is presented and ended with concluding remarks. Chapter 3, Methodology, describes the experimental procedures for this research. Details of the specimens and instruments are provided. Moreover finite element analysis will be carried out for simple verification purpose. Fatigue Analysis in Chapter 4 presents the experimental findings and discussion for the experimental work shown in previous chapter. Finally, Chapter 5 summarizes present work and provides recommendations for improvements and directions for future works.

1.5 Scope of work

This thesis mainly focuses on dynamic characteristic of rubbers. In order to have a clear understanding of the work, the scope is limited as follow:

(a) Materials and specimens:

The materials used are Natural Rubber (NR) with two carbon black contents: 10wt% and 25wt% respectively.

(b) Three geometries of rubber specimens will be used:

   (i) ASTM D-412C dumbbell shape specimens

   (ii) Specially designed shear specimens

   (iii) Specially designed diabolo specimens

(c) Mechanical testings:

   (a) Uniaxial tensile tests on ASTM D-412C dumbbell shaped specimens to investigate general macroscopic mechanical response.

   (b) Fatigue testing on shear specimens and diabolo-shaped specimens to obtain the fatigue behavior of elastomer under multiaxial loading condition.

   (c) Modal analysis to investigate the vibration characteristics.

CHAPTER 2: LITERATURE REVIEW

This chapter summarizes important and relevant information obtained from the literature including earthquake vibration isolator system, general characteristics of elastomers, mechanical responses of elastomers and fatigue behaviour of elastomers.

2.1 Earthquake vibration isolator system

A secure shelter is a basic requirement for a civilised society other than food and clothing. Conventional design of a structure is used to support vertical loads with low resistance to lateral forces. High rise buildings are especially prone to vibrations in the form of wind and seismic loading. The situation may be even worse when structures encounter harsh conditions caused by natural disasters (Irwin & Breukelman, 2001).

Among various natural disasters, from floods and cyclone, earthquake is one of the major cause of loss and casualties worldwide. During an earthquake, a sudden energy released from the Earth's crust. Wave passes through the Earth and impart motion to the ground, causing seismic vibration. Strong seismic forces transmitted from substructure to superstructure. Without any seismic protection, concrete buildings which experiences vigorous vibration from the ground may collapse (Kelly & Konstantinidis, 2011; Murty et al., 2012).

The damage of earthquake is often seen in last few decades. One of the most damaging earthquake has happened in China in the year 2008, which involve fatalities property loss. The damage is indeed worsen with the collapse of chemical plant (Mannan, 2013). Japan, which is one of the earthquake prone country experienced a number of severe earthquakes. Among the most damaging earthquake occurred in the year 2011, known as Tohoku earthquake was estimated with a magnitude of 9.1. This devastating earthquake causes large number of casualties, destructive on the houses and infrastructures. Thus, it is important to overcome the effect of earthquake especially on skyscrapers, hospitals, chemical plants to reduce the harmful effect of earthquake to the environment. This promotes the extensive study of earthquake protective systems.

Study on earthquake protective system is not a new subject up to date. Many systems are available currently to resist earthquake phenomena on structural buildings (Castaldo, 2014). The major advantage of the system is that it can protects all the elements within the isolation plane. It reduces the accelerations encountered from inertia forces of the structure and also the attachment such as water tank or plant items as well. Ideally, the invention of energy dissipation device is to reduce the structural forces by shear deformations. With the aid of the earthquake prone device, the building experiences less damage and is more likely to function normally immediately after occurrence of earthquake (Booth & Key, 2006).

Figure 2.1 illustrates the different force-deformation curves with and without energy dissipation system (EDS). The figure clearly shows the efficiency of energy dissipation system to overcome ground motion due to earthquake for metallic yielding, friction and viscoelastic systems. The curves shown are extended to the inelastic range. The addition of energy dissipation systems increases the strength and stiffness of the structure. Precisely, these systems increases the strength of structure by reducing drift and total lateral force exerted by earthquake vibration, thus reduces the deformation to levels below the elastic limit (Constantinou et al., 1998).

2.1.1 Basic principle of structure control system

Conventional anti-seismic approach relies on the capacity of the structure to resist inertia through the strength, deformability and energy absorption. The ability of the structure in damping is very low. Only small amount of energy is dissipated through elastic behaviour. When strong seismic excitation occurs, the structure could not dissipate seismic energy, thus deform beyond the elastic limit, resulting to a structural damage (Rai et

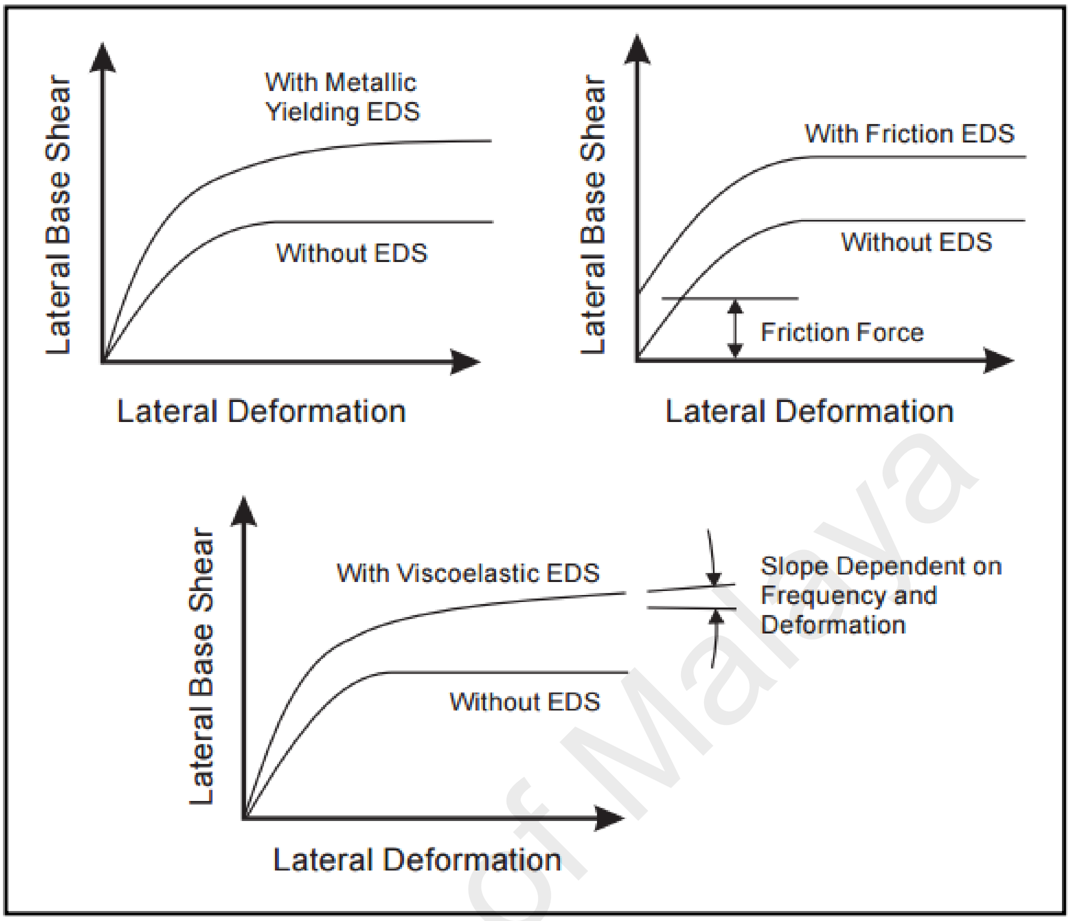

Fig. 2.1. Effect of energy dissipation on force deformation curves of a structure (Constantinou et al, 1998)

al., 2009).

From a mechanical point of view, earthquake energy distribution from the ground to the structure can be related in a time-dependent energy conservation relationship, given by,

$$E(t) = E_k(t) + E_s(t) + E_h(t) + E_d(t) \tag{2.1}$$

where $E(t)$ is the absolute energy input from the earthquake motion, $E_k(t)$ is the absolute kinetic energy, $E_s(t)$ is the recoverable elastic strain energy, $E_h(t)$ is the irrecoverable energy dissipated through inelastic, viscous and hysteretic actions, $E_d(t)$ is the energy dissipated by supplemental damping system and t is time (Soong & Spencer, 2000).

In the conventional structures without dedicated damping system, $E_d(t)$ is not present. Under excitation, the energy transmitted from the ground motion is transformed into kinetic and strain energy which are absorbed or dissipated through heat (Shrimali et al., 2015). Since energy dissipation capacity of a conventional structure is low, seismic energy is not able to dissipate through any means. Thereby, causing damage to the structure (Matsagar & Jangid, 2005). This situation can be minimised with a supplemental energy dissipation system which is able to absorb large portion of seismic energy instead of absorbed by the structure (Lewangamage et al., 2004).

2.1.2 Types of structure control system

Earthquake protective systems can be primarily divided into four categories, which include passive, active, semi-active and hybrid systems as shown in Figure 2.2. The details of each system can be explained as follow.

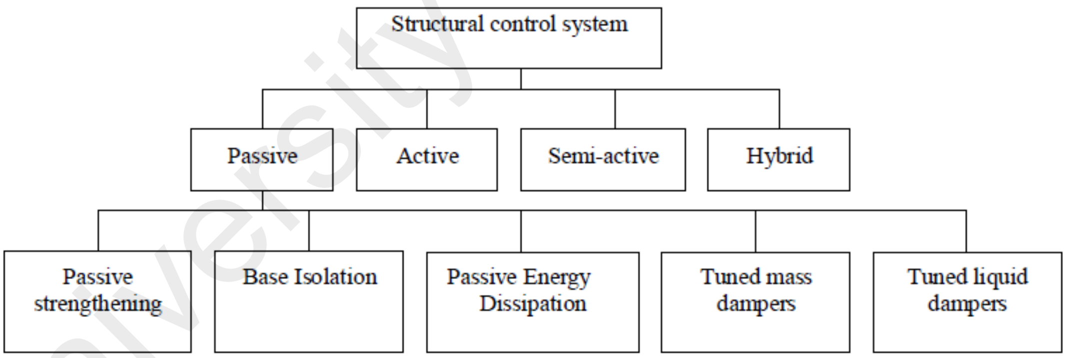

Fig. 2.2. Structure control system.

A passive control system consists of materials which enhances damping, stiffness and strength used in seismic hazard for rehabilitation of aging structures (Moreschi, 2000). Passive system devices generally operate on principle such as frictional sliding, yielding of metals, phase transformation in metals, deformation of viscoelastic solids or fluids (Soong & Spencer, 2002). The element of a passive energy system can be referred in Figure 2.3 (Soong & Spencer, 2002).

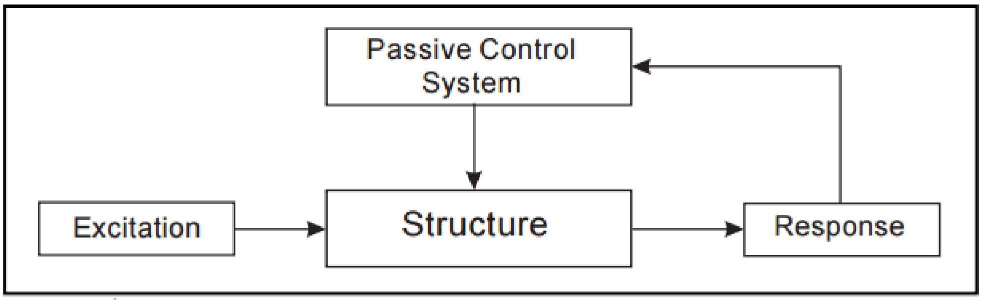

Fig. 2.3. Elements of a passive control system.

The main difference between a passive and other control system is that for active, hybrid and semi-active control system, processing controllers and sensors are attached within the structure (Symans et al., 2008). The system will be activated with hazardous excitation to protect the structure.

Active control system has the elements as shown in Figure 2.4. Generally it consists of:

1. sensors located at the structure to measure external excitations and/or structural response.

2. devices to process the measured information and to compute necessary control forces needed based on a given control algorithm.

3. actuators, powered by external sources to produce required forces.

A hybrid control system is typically defined as one that employs a combination of passive and active devices as shown in Figure 2.5. Because multiple control devices are operating, hybrid control systems can alleviate some of the restrictions and limitations that exist when each system is acting alone. Thus, higher levels of performance may be achievable. Additionally, the resulting hybrid control system can be more reliable than a fully active system, although it is also often somewhat more complicated (Soong & Spencer, 2002).

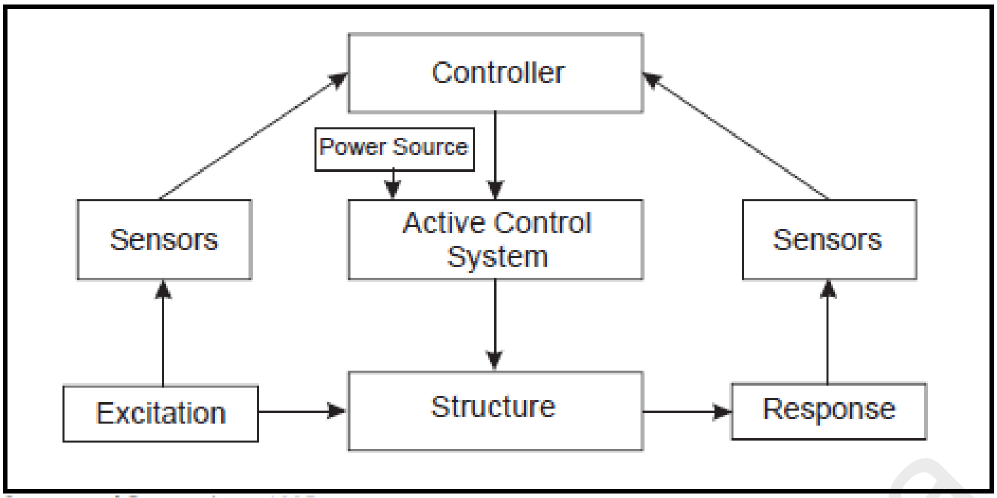

Fig. 2.4. Elements of a active control system.

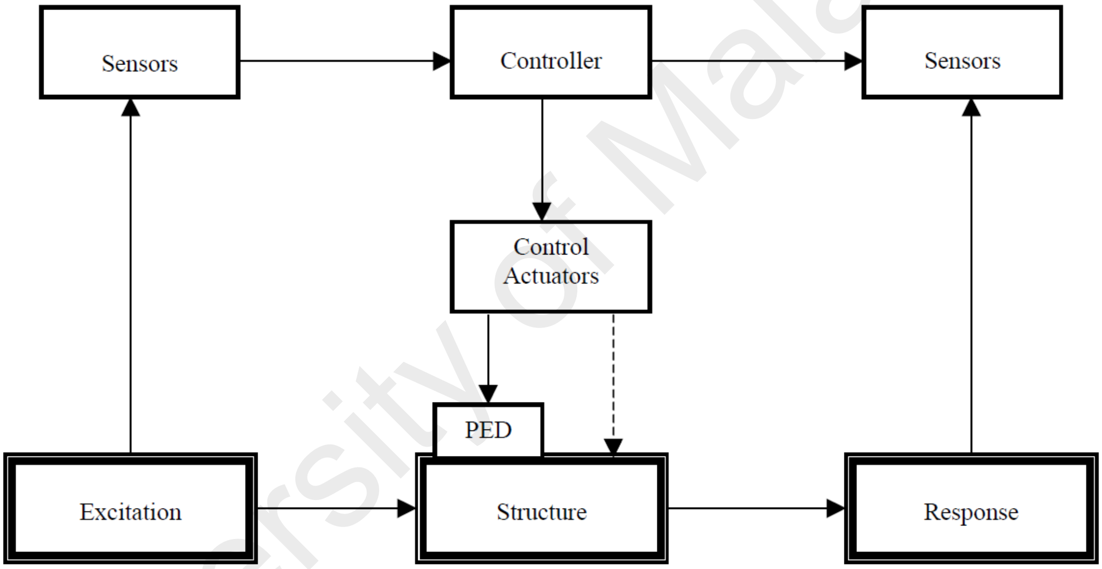

Fig. 2.5. Elements of a hybrid system.

Vibration control strategies based on semiactive devices combine the features of both passive and active control systems and to protect civil engineering structural systems against earthquake and wind loading. The attention received in recent years can be attributed to the fact that semiactive control devices offer the adaptability of active control devices without requiring the associated large power sources. In fact, many can operate on battery power, which is critical during seismic events when the main power source to the structure may fail. The elements of semiactive-system is shown in Figure 2.6.

Among the available systems, the most commonly used is passive system, which

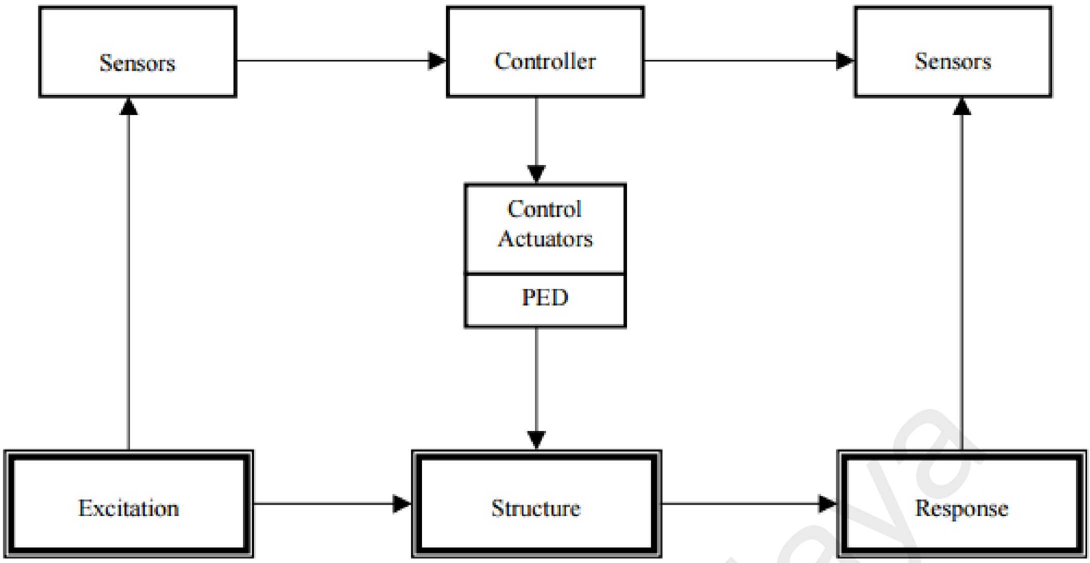

Fig. 2.6. Elements of a semi-active system.

includes seismic isolation and passive energy dissipation. Many studies has been done on seismic isolation where it has been widely developed (Iizuka, 2000; Topkaya et al., 2004; Kelly & Konstantinidis, 2011).

2.2 General characteristics of elastomers

Elastomer is an interesting material which exhibit excellent mechanical properties such as the ability to deform elastically at large strain, high strength and durability (Luksameevanish et al., 2006). This promotes the usage of elastomer in many engineering applications including engine mountings, tires, vibration isolators and structural bearings. Under these applications, the material undergoes various mechanical loading. Tensile, compression and shear forces are among the various conditions experienced on elastomers. The uniqueness of elastomer is able to return to its original configuration after the applied stress is removed. This generally can be described by the molecular aspect of elastomer, where high elasticity and the long chain polymer network with strong internal bonding able to resist the applied forces (Treloar, 2005).

2.2.1 Structure of elastomers

Elastomers are made up of a complex combination of polar and non-polar substances such as polymers, filler, oil, stabilizer, and curing agent by a series of processing method. Elastomeric materials posses a very high molecular weight. They are commonly composed of one or more monomers polymerized or co-polymerized together to form a polymer. These types of material are having low Young's modulus of elasticity and high yield strain (Abu-Abdeen, 2010). The structure of elastomer is illustrated as 'spaghetti' as there are multiple cross linking. It consists of a very long chain of monomer molecules chemically bonded together forming a single molecule. When subjected to stress, the molecules will be stretched. Cross linking between chains of molecules prevent further elongation of elastomer under loading. When the stress is released, the chain of molecules will return to their initial states.

Vulcanization process is done by mixing the vulcanization agent into the heated rubber and mold under pressure. Table below shows material formulations of different elastomeric material with different vulcanization time and temperature (Mark et al., 2013). Initially vulcanization was done by adding sulphur at concentration of 8 parts per 100 parts of rubber (phr). This process required 5 hours at 140. Addition of zinc oxide reduced the vulcanization time to 3 hours. Thus, this has resulted the introduction of accelerator during vulcanization for time and cost efficient especially in the industry. Organic chemical accelerator has been discovered which involves less toxic reaction product with carbon disulphide and thiocarbanilide. Delayed-action accelerators were introduced which results in delayed action but faster curing vulcanization (Nakason et al., 2006).

2.2.2 Types of elastomers

Elastomers can be classified into two categories, thermoset or thermoplastics. Thermosets is made up of polymer chains with chemical crosslinks. Upon heated, thermosets do not dissolve. Meanwhile thermoplastics are joined physical entanglements. Chains can be dissolved when heated and form a new product (Callister & Rethwisch, 2012).

Properties of natural rubber is only applicable for a limited number of application. In order to cope with more extreme application requirements, this led to the existance of several general purpose elastomers, for example ethylene propylene diene modified rubber (EPDM), polychloroprene (CR) and polysiloxane. The following gives details of these rubber properties.

(a) Natural rubber

Polyisoprene, or more commonly known as natural rubber (NR) is the world's first commercially produced elastomer. Sourcing from latex of the rubber tree Hevea Brasilienis, natural rubber is economic. Its low dynamic response, low hysteresis and high levels of durability makes a good material selection for anti-vibration dampers and elastomeric bearings. However, on the limitation side, its performance in high temperature and oil is unsatisfactory. Malaysia, being one of the largest natural rubber producer in the world has high contribution in rubber industry.

The effect of crystallization of NR on the fatigue life was investigated by many researchers (Le Cam, Huneau, & Verron, 2008; Rublon et al., 2014; Legorju-Jago & Bathias, 2002; Saintier, Cailletaud, & Piques, 2011; Lake, 1995; Mars & Fatemi, 2006; Huneau et al., 2016; Beurrot-Borgarino, Huneau, Verron, & Rublon, 2013; Santangelo & Roland, 1995; Chenal, Gauthier, Chazeau, Guy, & Bomal, 2007; Toki, Fujimaki, & Okuyama, 2000). Le Cam (Le Cam et al., 2008) described the different levels of strain experienced by natural rubber led to different type of fatigue damage. Under non-relaxing uniaxial tension, small surface crack at sample feet and crack branching due to the presence of crystallites were observed. This contributes to the improvement of the rubber fatigue life.

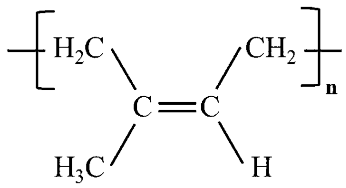

Fig. 2.7. Chemical structure of polyisoprene.

(b) EPDM

Ethylene propylene diene modified rubber, (EPDM) formed by the combination of both ethylene and propylene monomer, resulting saturated and stable polymer backbone. This structure gives EPDM excellent resistant to heat, ozone, oxidation and weather aging, which is applicable in construction, mechanical goods and automotive industry.

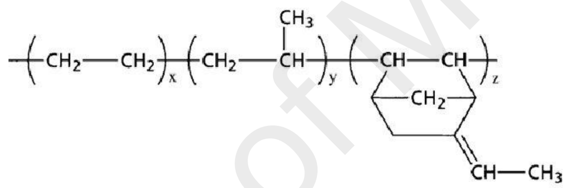

Fig. 2.8. Chemical structure of EPDM.

(c) Polychloroprene

Polychloroprene rubber (CR) is also known as “Neoprene” as the trade name in the industry. CR is widely used in rubber industry. Various products are produced using CR, such as moulded goods, cables, transmission belts and conveyor belts. CR is favorable due to several characteristics which includes good mechanical strength, high ozone and weather resistance, good aging resistance, low flammability, good resistance toward chemicals, moderate oil and fuel resistance and adhesion to many substrates.

CR has been used by Berton et al (Berton, Cruanes, Lacroix, Méo, & Ranganathan, 2015), Poisson et al (Poisson, Lacroix, Meo, Berton, & Ranganathan, 2011), Suryatal et al (Suryatal, Phakatkar, Rajkumar, Thavamani, et al., 2015), and Marco et al

(Marco, Le Saux, Calloch, & Charrier, 2010). Berton et al (Berton et al., 2015) observed that the stiffness of the rubber decreases when subjected to increasing phase of force ratio. During the decreasing phase, strain-induced-crystallization occur at the cracked site thus increases. Berton and his team concluded the evolution of hysteresis and stiffness indicated the effect of strain-induced-crystallization of polychloroprene.

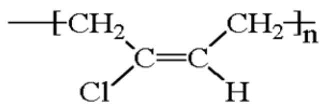

Fig. 2.9. Chemical structure of polychloroprene.

(d) Polysiloxane

Polysiloxane or silicone rubber, differ from other type of rubber which mainly consist of carbon backbone, it is made up of siloxane backbone. The significant difference is the flexibility of the backbone in silicone rubber and higher binding energy. These results in higher heat resistant and chemical stability.

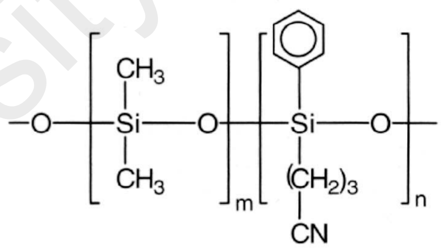

Fig. 2.10. Chemical structure of polysiloxane.

2.2.3 Reinforcement

Without reinforcement added to the rubber matrix, it is impossible for elastomer to withstand high stress during the service. The significance of reinforcement is to improve in abrasion, tear, cutting and rupture resistance, in stiffness and hardness of vulcanized compound through the incorporation of finely divided particles (Mostafa et al., 2009). Several additives which commonly used in the industry will be discussed below.

2.2.3 (a) Carbon black

One of the examples of reinforcement is carbon black which appears in the form of powder. It is used in tires, rubber and plastics products to enhance the material's properties and to have a longer lifetime (Park Kim, 2001). Anti-vibrating structure, for example, is made from natural rubber reinforced by carbon black. Addition of carbon black into natural rubber compound greatly affects the overall mechanical properties. Elastic modulus and tensile strength has improved significantly, while sharp increase of hysteresis can be expected in the system (Donnet, 2003).

The work on investigating the effect of carbon black on elastomer is widely done in recent years. Study on the variation in amount of carbon black is done by Luksameevanish et al. (2006) to investigate the effect of carbon black on bearing behavior. In practical, higher amount of carbon black will be used as sufficient amount of carbon black is able to give significant mechanical improvement. This can be seen in figure below.

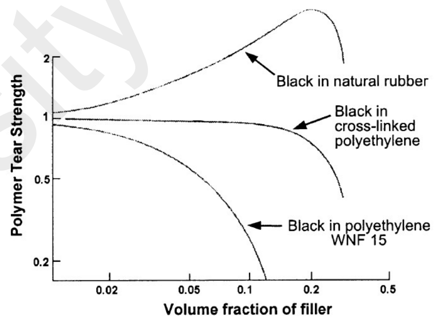

Fig. 2.11. Filled polymer tear strength (Donnet,2003).

Three materials with different contents were compared, which is unfilled, graphitized and reinforced carbon black samples (Mark et al., 2013). Unfilled rubber showed weaker property compared with the other two. Among these three materials, reinforcing carbon black sample has highest stress-strain curve. This proves that addition of carbon black in materials will have significant changes on materials (Sirisinha & Prayoonchatphan, 2001).

Addition of carbon black in different type of polymer is done in the work of Donnet (2003). With the same volume fraction of filler added into natural rubber, cross-linked polyethylene and polyethylene WNF 15, natural rubber shows highest polymer tear strength. The improved strength properties, stiffness, abrasion and tear resistance may governed by the carbon black particles (Xie et al., 2005). Via STM microscopy, carbon black particles are rough "scale" of carbon graphitic organization (Donnet, 2003). The existence of "active sites" at the edge shows the interactions between the surface and elastomeric chains. This active sites serves as stronger connection site with the material compounds (Omnès et al., 2008).

2.2.3 (b) Fire retardant agent

Fire retardant agent is useful in many applications to minimize fire hazard. The invention of fire resistant elastomer is useful in aircraft seat cushions. The materials used to produce the seat cushions are polyurethane and polyphosphazene elastomers with expandable graphite flakes added in the elastomeric compound. As a result, the peak heat release rates are reduced by five to seven times (Lyon et al., 2003). Thus, the usage of fire retardant can also applicable in base isolator system. Buildings are prone to fire hazard as there are complicated electrical wiring system and materials which accelerate fire combustion. Base isolation system with fire resistant agent may reduce the chance of the entire building collapse thus reducing loss.

According to the review done by Kind (2012), natural rubber without fire retardants have low resistant to burning. On top of that, it emits large quantities of dense smoke. Detailed mechanism of thermal decomposition of natural rubber can be described by random chain scission upon heating. This lead to vaporizing into a mixture of small aromatic chemical species, which ignite readily and form smoke particles with negligible char residue formation (Kind & Hull, 2012). Natural rubber is a widely used material in various industry, under various conditions. Since the effect of natural rubber in thermal composition is poor, therefore fire retardant additives should be introduced. Based on Kind (2012), cross-linking agents have significant effects on physical and ageing properties, however they are do not have much effect on thermal decomposition and burning. In this study, the reviewed fire retardants are halogenated additives, high loadings of aluminium hydroxide (ATH) where both do not show satisfying result. Phosphorus and nitrogen based additives as intumescent char formers, with zeolites as char catalyst are identified. Inorganic fire retardants such as zinc hydroxystannate and zinc borate have similar effect as ATH. Expandable graphite (EG) is identified material used in other elastomes, which may has potential for natural rubber.

2.3 Mechanial responses on elastomers

Unlike other materials, elastomers exhibit different responses when subjected to mechanical loading. Several phenomena such as hysteresis, stress-softening and permanent set occur when elastomer are subjected to mechanical loading. In this section, mechanical response of elastomers under monotonic and cyclic loading are discussed.

2.3.1 Mechanical behaviour of elastomer under monotonic loading

Under monotonic loading, where force is applied slowly, the elastomeric material will experience non-linear elastic response or known as hyperelasticity. Hyperelastic constitutive laws are used to model materials that respond elastically when subjected to very large strains. Elastomers returns essentially to its original shape after the load has been removed.

Different materials exhibit different stress-strain curves as shown in Figure 2.12. Brittle material which is in glassy state is able to withstand high stress but rupture at low strain. Plastic failure occur at lower stress after plastic deformation takes place. Elastomer is able to withstand high strain due to its polymer chain arrangement.

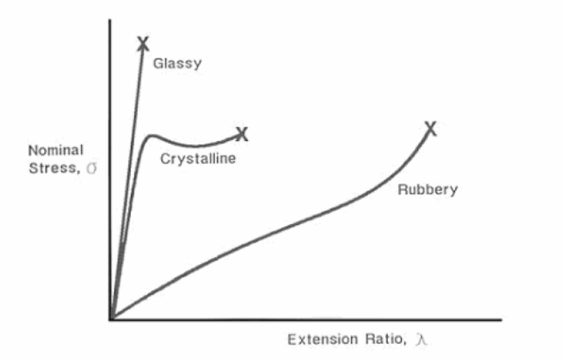

Fig. 2.12. Tensile stress-strain curves for polymers in three different physical states, X denotes rupture, Gent(2012)

2.3.2 Mechanical behaviour of elastomer under cyclic loading

Special characteristics of elastomer can be observed from the stress-strain graph of elastomer, as it exhibits inelastic behaviour when subjected to cyclic loading. A few commonly occurred behaviour are hysteresis, permanent set and stress-softening which is presented in Figure2.13 (Stevenson, 1983). Figure 2.13 shows the mechanical loading condition when a carbon black filled rubber is subjected to simple uniaxial tension test and cyclic uniaxial tension test (Diani et al., 2009).

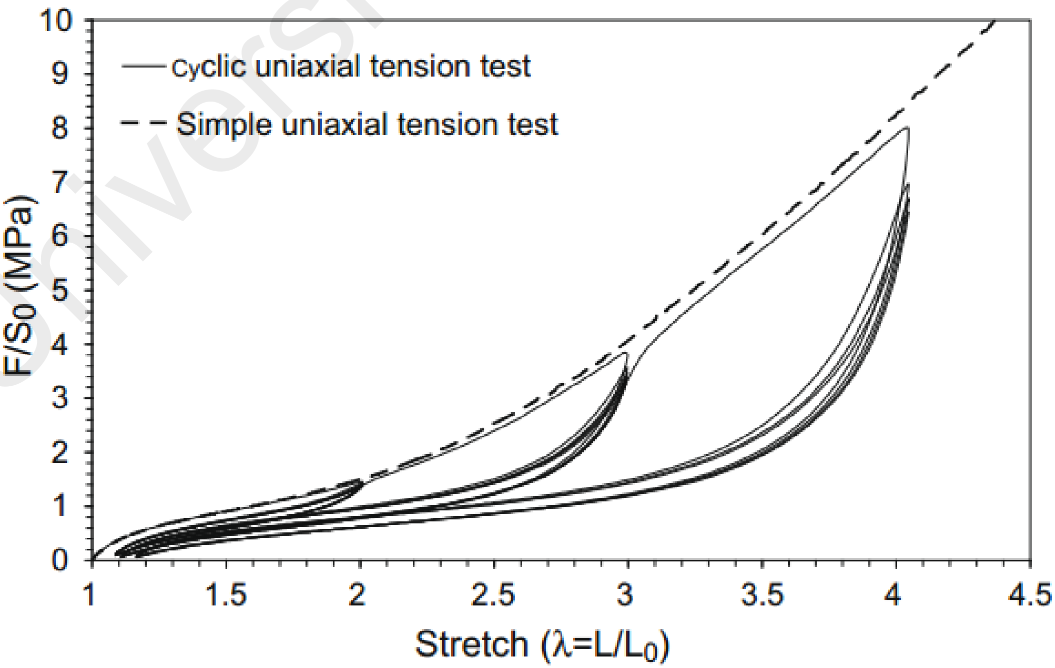

Fig. 2.13. Stress–strain responses of a 50 phr carbon-black filled SBR submitted to a simple uniaxial tension and to a cyclic uniaxial tension with increasing maximum stretch every 5 cycles (Diani et al.,2009).

2.3.2 (a) *Hysteresis*

The hysteresis is identified as an appearance of a loop in the stress-strain curves when the material is subjected to a cyclic loading. While hysteresis is commonly related to heat dissipation, Martinez and his co-workers (Martinez et al., 2015) found that hysteresis loop in unfilled NR can also be observed in the mechanical response without any intrinsic dissipation. Hysteresis loss increases with increasing strain rate, filler loading, resin loading, crosslink density and strain level resulting larger loop in the stress-strain curve. Conversely, it decreases with increasing temperature, particle diameter of filler and resin loading at high testing temperature (Kar & Bhowmick, 1997). Under cyclic mechanical loadings, the hysteresis is significantly larger for the first loading cycle and subsequently the amount of hysteresis reduces and stabilizes (Yamaguchi et al., 2003).

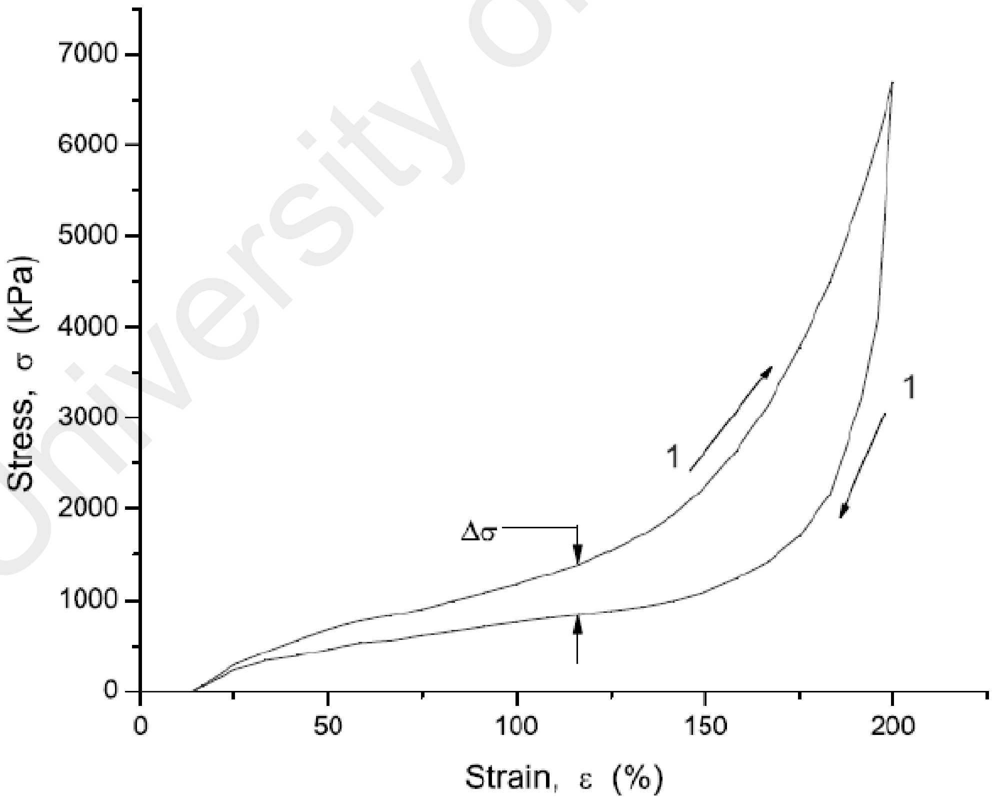

Fig. 2.14. Cyclic loading of tensile specimen exhibiting hysteresis (Bauman, 2008).

2.3.2 (b) Mullins effect

Stress-softening is another phenomenon observed during cyclic loading of elastomer. Also known as Mullins effect, this phenomenon was firstly observed by Bouasse & Carriere (1903) and was further studied by Mullins (1948). The Mullins effect is characterized by the decrease of the stress level in both the uploading and unloading during the first couples of loading cycles. After several loading cycles, the stress-strain response stabilizes and the following loading cycles merely retrace the path of the stabilized stress-strain curve (Mars, 2001).

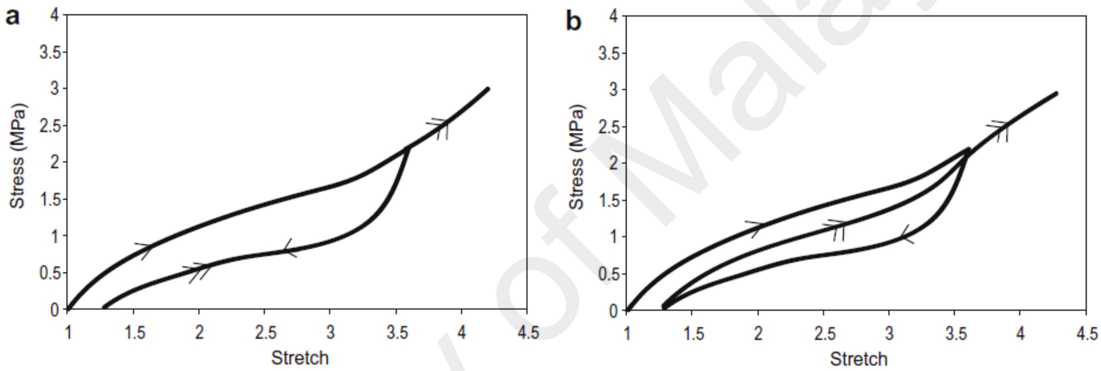

Fig. 2.15. Model representation of the mechanical behavior of rubbers undergoing Mullins softening. (a) First class of models: reloading response coincides with the unloading response and (b) second class of models: the reloading and the unloading responses differ.

2.3.2 (c) Permanent set

Permanent set is a phenomenon where after an elastomeric material is being loaded and unloaded, there is residual strain. This occurs due to the resistance of the new bonds formed by the rupture chain segments from the deformation when the material is released back to the original shape. The effect of permanent set decreases slowly with time and eventually disappears after a period of time (Dorfmann & Ogden, 2004). A few factors that affect the occurrence of permanent set, such as the amount of carbon black, the maximum elongation loaded on the elastomer and the duration of the material under deformed state. The magnitude of permanent set for unfilled elastomers is relatively small and often negligible. However, for filled elastomers the effect is significant and increases with the amount of filler in the elastomer (Lion, 1996). Permanet set can be observed clearly under cyclic loading, during the first unloading cycle. The magnitude of permanent set will continue to increase for a number of cycles until a constant value is reached (Zarrin-Ghalami & Fatemi, 2013).

2.4 Factors affecting fatigue behaviour of elastomers

Lifetime of elastomers greatly varies depending on several factors, mainly rubber formulations, loading conditions and environmental conditions. By varying each factor, the resulting fatigue response will be different. Gaining understanding on the influence of fatigue life of rubber aids in choosing the optimum rubber in service (Mars & Fatemi, 2002).

2.4.1 Rubber formulation

Mechanical properties of rubber can be altered by changing the rubber formulation and manufacturing process. Apart from the major rubber content, either natural or synthetic, rubber compound consists of antioxidants, antiozonants, fillers, curing agents and processing aids to improve the performance of rubber in application (Mark et al., 2013). The manufacturing process also plays important role in producing higher durability rubber. Dispersion of ingredients in a rubber compound, state of cure and the existent of sites for crack initiation may significantly affect the lifetime of rubber (Mohammed et al., 2014; Smallwood, 1944).

Type of polymers is one of the factor that impact the behavior of fatigue. Some polymers exhibit strain crystallization which can withstand high mechanical loading and good fatigue performance. They are less susceptible to environmental damage (Mars & Fatemi, 2004b). Several examples of strain-crystallized polymers are natural rubber (NR), isoprene rubber (IR) and polychloroprene (CR). On the other hand, polymers that exhibit little or no crystallization are styrene-butadiene rubber (SBR), polybutadiene (BR), butyl rubber (IIR), acrylonitrile-butadiene rubber (NBR) and ethylene-propylene rubber (EPDM) (Merckel, 2012).

The addition of carbon black significantly strengthen elastomer. The mechanical effect of filler contributing to elastomer include:

1. Improved in stiffness and hysteresis properties
2. Crack tip blunting, deviation and branching due to nonhomogeneity of the rubber-filler composite
3. Agglomeration of filler particles, resulting in increased effective initial flaw sizes

Although the idea of introducing filler into rubber compound brings positive effect, however the filler type and volume fraction used is another issue to be noted. With an optimal filler added into the rubber compound, this minimizes crack growth rate. Below the optimal volume fraction, the reinforcement result in improved fatigue life. Above the optimal volume fraction, it causes increase in initial flaw size, resulting reduced fatigue life (Auer et al., 1958).

In the work of Klüppel (Klüppel, 2009), the fatigue crack propagation behaviour was compared between two types of fillers, silica and carbon black in SBR. It was observed that the filler-filler bond increased with carbon black content. Compared to carbon black, silica formed less stable filler cluster which results in lower hysteresis and tensile strength. Dong et al (Dong, Liu, & Wu, 2014) studied the fracture and fatigue of NR filled with varied silica and carbon black content. It was found that the addition of silica improved the crack initiation and propagation resistance, resulting in longer lifetime. Ismail et al (Ismail, Muniandy, & Othman, 2012) investigated fatigue life of rattan powder-filled NR. The fatigue life of the material decreases with increasing rattan powder content in thermal aging test. They showed that there was decrease in tensile strength and elongation at break, while increase in tensile modulus and stress.

According to Diani et al. (2009), comparison between 50 phr carbon black filled and unfilled natural rubber was made. It was noticed that filler act as strain amplifier. As a result lower strain level is noticed in filled natural rubber than unfilled natural rubber under equivalent stress applied. Thus rubber with filler such as carbon black enhances its property under mechanical loading, resulting longer service life than pure rubber formulation.

2.4.2 Loading conditions

Mechanical loading history is one of the factor affecting the durability of a material. Several parameters such as maximum, minimum, alternating and mean loading need to be characterized (Le Cam et al., 2008). One of the most significant characteristics of elastomer in cyclic loading is the maximum load applied resulting Mullins effect. The lifetime of elastomer may be longer subjected to lower maximum load compared to higher maximum load. Meanwhile, the effect of mean loading is depending on the type of elastomer and filler used. Natural rubber, which exhibit strain crystalization, the durability can be improved with increase in the minimum strain and constant maximum strain. It should be noted that this condition does not applied to non-crysallizing elastomers (Mars & Fatemi, 2002).

Abraham et al (Abraham, Alshuth, & Jerrams, 2005) investigated the effect of maximum and minimum stress amplitude for non-crystallizing rubber. They found that increasing minimum stress with constant strain amplitude greatly increases the service life of the filled rubber materials. While researchers generally focused on constant amplitude loading conditions (Ghosh, Mukhopadhyay, & Stocek, 2016; Zhou, Jerrams, & Chen, 2013; Saintier, Cailletaud, & Piques, 2006a), Harbour et al (Harbour, Fatemi, & Mars,

2008) proposed the study of fatigue behaviour of rubber under variable amplitude and multiaxial loading conditions as it represented actual applications during service. Comparing NR and SBR, crack appearance in NR is more than SBR. The increase of fatigue life is related to the rubber fillers system. On the contrary, strain crystallizing is the common contribution to fatigue life in strain crystallizing rubbers.

Besides displacement control, some researchers have conducted tests under stress control loading conditions. Legorju-Jago and Bathias (Legorju-Jago & Bathias, 2002) examined the effects of load ratio on the lifetime of different rubbers. The load ratio is defined as the maximum load over the minimum load. The compression loading, where $R = -1$, caused damage to NR because reinforcement due to crystallization did not occur. Similarly, Ghosh et al (Ghosh, Stocek, Gehde, Mukhopadhyay, & Krishnakumar, 2014) showed that positive R ratio resulted significant decrease in crack growth rate for the NR specimens. El and Altstädt (El Fray & Altstädt, 2003) investigated fatigue behaviour of thermoplastic and silicone rubber under stress controlled loading condition the material exhibited great fatigue lifetime compared to silicone rubber due to its higher dynamic modulus.

In fatigue testing, the rubber material tend to self-heat due to its low thermal conductivity. Consequently, increasing the frequency should be avoided when it increases the surface temperature of rubber. Indeed, it was reported that the lifetime of NR was shortened when crystallization was hindered due to high temperature (Candau et al., 2015). Self-heating of rubber NR has been explored in the work by Stadlbauer et al (Stadlbauer et al., 2013). Moreover, Stadlbauer and her team (Stadlbauer et al., 2013) found that the frequency range between 1-5Hz is not important unless self-heating exceeded the temperature limit.

The relationship of crack growth with the maximum energy release rate, R can be illustrated as shown in Figure 2.16. For a rubber component under cyclic loading, it is possible to experience four different stages: a sub-threshold regime, a transition regime, a power-law regime and a failure regime which unstable crack growth occurs.

In the initial stage, where the maximum energy release rate, R=0, it shows that the load applied is below the mechanical threshold. There will be no cracks observed due to cyclic mechanical loading. However other factors such as environmental issue may still take part in the crack growth process under this stage.

When the applied load is above the threshold required for mechanical crack growth, but remains below the critical value, the rubber is in the power-law regime. In this stage, it is common to notice crack nucleation and crack growth.

When subjected to a critical load, fatigue crack growth rate increases rapidly to unstable fracture. For a non-crystallizing rubber, failure may occur at any time. However, for crystallizing rubbers at high strains, the material may crystallize before the point of unstable crack growth. The strength of this material can be increased by more than a factor of two (Lake & Lindley, 1964).

Rubber in practical involves multiaxial mechanical loading. However, mechanical behavior of multiaxial mechanical loading are not fully understood up to date (Le Cam, Huneau, & Verron, 2013). Although with current simulation technology it is possible to predict the multiaxial loading histories, however the ability to predict fatigue life from computed loading histories is still lacking (Mars & Fatemi, 2002). More research work is needed in this area.

2.4.3 Environmental conditions

Environmental conditions play an important role in determining the lifetime of rubber under application. Apart from multiaxial mechanical loading, the surrounding of the rubber component may affect its serving time.

Temperature is one of the cause of reduction in service life of a rubber component.

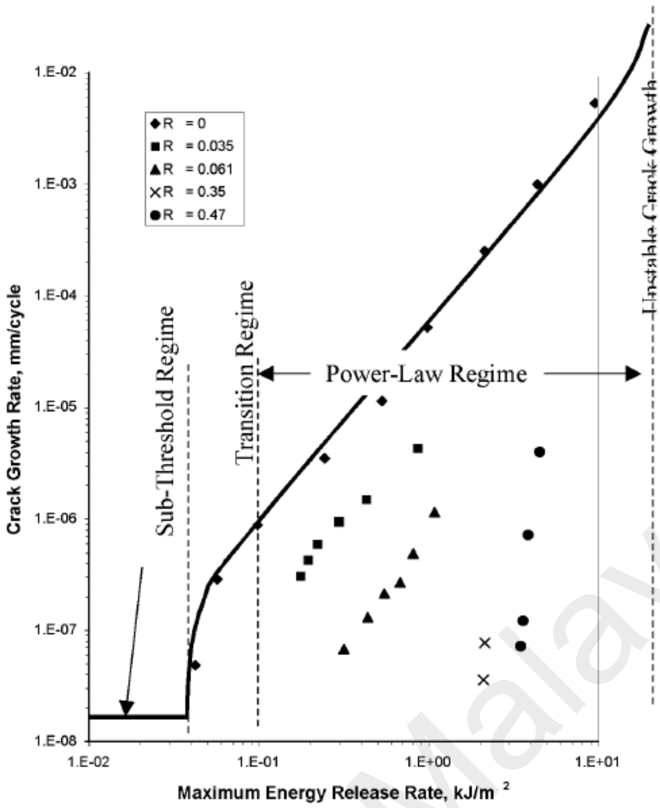

Fig. 2.16. Lindley's fatigue crack growth results for unfilled natural rubber, showing typical regimes of behaviour, and the effects of R> 0 loading.

This effect is prominently seen in amorphous rubbers. Under an experimental test, for gum SBR, the fatigue life drops by a factor of 10^4 with the temperature increases from 0°C to 100°C. However, the degradation effect is lesser for gum NR, with the fatigue life drops by a factor of 4. This should be noted that the influence of temperature on fatigue life may varies with rubber formulation such as fillers, curatives and antioxidants.

Apart from temperature, long-term exposure to ozone significantly increases crack growth rate and reduces the lifetime of rubber(Lake & Lindley, 1966; Braden & Gent, 1960). From molecular point of view, ozone reacts with carbon bonds in the main polymer chain, which causes chain scission thus resulting fractures (Hon et al., 2003).

Fatigue of rubber in air has been extensively studied, and oxygen played an important role. Le Gorju and Bathias (Legorju-Jago & Bathias, 2002) found that NR experienced chemical damage due to the presence of oxygen in the air. The condition is extended to high temperature and oxidation reaction occurred rapidly. This situation differs when NR is exposed to nitrogen and water. Temperature effect on the lifetime of rubber is a concern as deterioration may occur when the material is used above its optimum temperature. Le Gorju and Bathias (Legorju-Jago & Bathias, 2002) found that crack growth rate of NR increased when the temperature was higher. The crystallisation of NR was greatly affected when the temperature was increased. Rey et al (Rey, Chagnon, Le Cam, & Favier, 2013) investigated the effect of temperature on filled and unfilled silicone rubber. Stiffness of unfilled silicone rubber increases with increasing temperature as the microstructure was stabilised. For filled silicone rubber, the hysteresis, stress relaxation and stress softening decrease with increasing temperature. Ismail et al (Ismail et al., 2012) showed that mechanical property of rubber was improved after thermal aging. On the contrary, experimental works based solely on EPDM by Chou et al (Chou, Huang, & Lin, 2007) found that the fatigue life of the rubber of both with and without carbon black filled was dramatically reduced after six months of thermal aging. Increase in aging temperature and aging time caused significant decrease in fatigue (Ngolemasango, Bennett, & Clarke, 2008). Ngolemasango et al (Ngolemasango et al., 2008) explained that strain crystallization characteristic of NR is inhibited when exposed to high temperature, resulting the increase in fatigue crack growth rate. Moreover, during aging process, antioxidants added in the rubber compound are depleted. This allows oxidative aging to occur, causing hardening at the rubber surface. While undergoing fatigue loading, cracks can be easily formed leading to failure in short duration.

While it is well-known that temperature affects the lifetime of rubber, the condition is worsen with the presence of oxygen as chemical-aging takes place (Lion & Johlitz, 2012). Several works (Johlitz & Lion, 2013; Lion & Johlitz, 2012; Herzig, Johlitz, & Lion, 2015) elucidate the characterization of thermo-oxidative aging characterization. Neuhaus et al (Neuhaus et al., 2017) conducted an experimental work to identify the aging effect with the combination of elevated temperature and oxygen. They found that thermo-oxidative aging increases the temperature sensitivity of rubber. In addition, the temperature sensitivity increases linearly with aging time.

Meanwhile, ozone is known to deteriorate rubber (Mars & Fatemi, 2004a). Vinod et al (Vinod, Varghese, & Kuriakose, 2002) found that ozone resistance of NR is improved with the addition of aluminum powder. Although cracks are observed on the specimen under the exposure of ozone, aluminum filled NR specimens have smaller and discontinuous crack compared to unfilled NR specimens. Saharako et al (Sahakaro, Talma, Datta, & Noordermeer, 2007) studied the effect of ozone on NR/BR/EPDM blend. It was shown that the presence of EPDM in the rubber compound improves the ozone resistance compared to NR/BR blend compound. Similarly, Sae et al (Sae-Oui, Sirisinha, & Hatthapanit, 2007) investigated the properties CR/NR blend. It was found that higher CR content in the blend improves both the mechanical properties and environmental resistance. Double bonds in the structure of NR made it susceptible to ozone attack. However, when suitable compound is added into NR formulation, it will greatly improve its ozone resistance property (Vinod et al., 2002).

Experimental works have been conducted to understand further the lifetime of rubber component in marine environment. Le Gac et al (Le Gac, Arhant, Davies, & Muhr, 2015) studied the fatigue behaviour of NR rubber in marine environment. They concluded that there was no difference in the mechanical response of rubber in marine and air under relaxing loading condition. However, decreasing lifetime was observed when the specimens underwent non-relaxing loading. This phenomenon was related to the reduced effectiveness of strain induced crystallization of the rubber which contributed to the lifetime. Effect of load ratio of rubber in marine environment was further studied by Ulu et al (Ulu, Huneau, Le Gac, & Verron, 2016). Although it showed similar trend under relaxing loading condition by Le Gac et al (Le Gac et al., 2015), there was a contradiction of results for rubber under non-relaxing loading condition. They observed that the lifetime of rubber improved when load ratio increased and was supported by other studies (Cadwell, Merrill, Sloman, & Yost, 1940; Saintier, Cailletaud, & Piques, 2006b; Saintier et al., 2011).

Moreover recently, it is established that the service life of elastomer is significantly affected by the exposure to aggressive liquid such as palm biodiesel (M. S. Loo et al., 2015; M. Loo et al., 2016).

2.5 Strain amplification factor

Filler is introduced into elastomer to improve mechanical properties such as tensile strength and resistance to abrasion, tear, fatigue and cracking (Voet, 1980). The addition of filler may have large effect on the elastomer compared to unfilled elastomer, particularly the inelastic response such as Mullins effect, hysteresis and stress relaxation.

Several literatures have been discussed about the effect of mechanical response with the introduction of fillers in terms of microscopic level. From molecular level standpoint, filler increases the crosslink density as the additional crosslinking takes place at the filler-matrix interface (Bueche, 1960). The movement of rubber matrix is restricted around the area of filler particles (Kraus, 1978). The effect of filler on the mechanical properties of elastomer may be affected due to the geometry of filler, such as the size, shape and structure (Mullins, 1950).

On the other hand, the existence of filler in elastomeric matrix has introduced a phenomenon, named as strain amplification. This theory is meant for composite system, for example, elastomer with filler particles. Fillers are considered as rigid particles which do not involve in the deformation when subjected to macroscopic stretch of the elastomeric material (Stevenson, 1983). Elastomeric matrix around the filler particles experienced higher stretch in microscopic view as the fillers do not deform. Addition of filler into elastomeric matrix caused amplified localised stretch, thus studies on strain amplification factor is discovered.

For uniaxial tensile stress-strain behavior, the amplified axial stretch is given by Guth and Simha (1936):

$$\lambda_{loc} = 1 + \chi(\lambda_{glo} - 1) \tag{2.2}$$

where χ is the strain amplification factor which depending on filler volume fraction, shape and distribution in the matrix while λ_{glo} and λ_{loc} is the macroscopic and microscopic axial stretch respectively.

The initial idea of amplification factor came from the Einstein's theory, a theory for the stiffening of elastomers by as rigid filler for the increase in viscosity of a suspension due to the presence of spherical colloidal particles (Einstein, 1905).

$$\hat{\eta} = \eta_o(1 + 2.5\phi) \tag{2.3}$$

where, η is the viscosity suspension, η_o is the viscosity of the incompressible fluid and ϕ is the volume fraction of the spherical particles.

This theory has been further studied by Smallwood (1944), Guth and Gold (1938) and Nielsen (1966). According to Smallwood (1944), the amplification factor of fillers in the elastomeric matrix is similar to the enhancement of viscosity of liquids. Therefore the elastic modulus is given by:

$$\hat{E} = E_o(1 + 2.5v_f) \tag{2.4}$$

where $\hat{E}$ and E_o are the elastic moduli of the filled and unfilled elastomer respectively and v_f is the filler volume fraction.

Equation 2.4 is well fitted for the elastomers containing low volume fraction of filler

(v_f <0.1) but for higher volume fraction of filler, large deviation is observed. Modification is needed for the model, thus Guth (1945) suggested that it can be improved by considering the interactions between surrounding filler particles and the proposed model is as below:

$$\hat{E} = E_o(1 + 2.5v_f + 14.1v_f^2) \tag{2.5}$$

Apart from the amplification factor proposed by Einstein (1906) and Guth and Gold (1945), Nielsen (1966) has derived an equation to describe the elongation from the microscopic view and the observed elongation, given by,

$$\hat{\varepsilon} = \varepsilon_o \left(\frac{1}{1 - v_f^{1/3}} \right) \tag{2.6}$$

where $\hat{\varepsilon}$ is the actual microscopic elongation and $\varepsilon_\circ$ is the observed elongation.

2.6 Summary

Several research gaps have been identified which are worth to be explored.

Four categories of structural control systems are available, including active, semi-active, hybrid and passive system. Passive systems are the most widely used, which works on damping principle. Base isolator which made up of rubber and metal plates gives promising efficiency. The implementation is required prior to the building constructions. Located in earthquake safe zone, some of the buildings do not equipped with structural control systems. Alternative devices are required for the buildings without earthquake protection system.

Research works on fatigue of rubber have been widely explored from various aspects. Fatigue characteristics of carbon black filled rubber are available in the literature, however, no works are carried out to explicitly consider the carbon black content. Strain amplification factor theory of Guth-Gold and Nielson is able to describe microscopically the effect of filler during mechanical loading.

CHAPTER 3: METHODOLOGY

A major part of the present work focuses on the experimental program. This includes the experimental procedures and materials used to perform the testings. More precisely, the mechanical behavior of elastomeric materials having different carbon black contents subjected to uniaxial and multiaxial cyclic loading will be investigated. Three types of specimens will be used in the testing to cope with different mechanical testings. Among the three geometries, one is according to the ASTM D-412C standard dumbbell shape specimen while the remaining two specimens are specially designed specimens, shear and diabolo shaped specimens. Natural rubber will be considered throughout the experimental work due to the wide use in damper system.

Next, a minor part of the work is dedicated to the modelling of the proposed sliding rubber damper (SRD) system.

The methodology of the work is summarized as shown in the flow chart Figure 3.1.

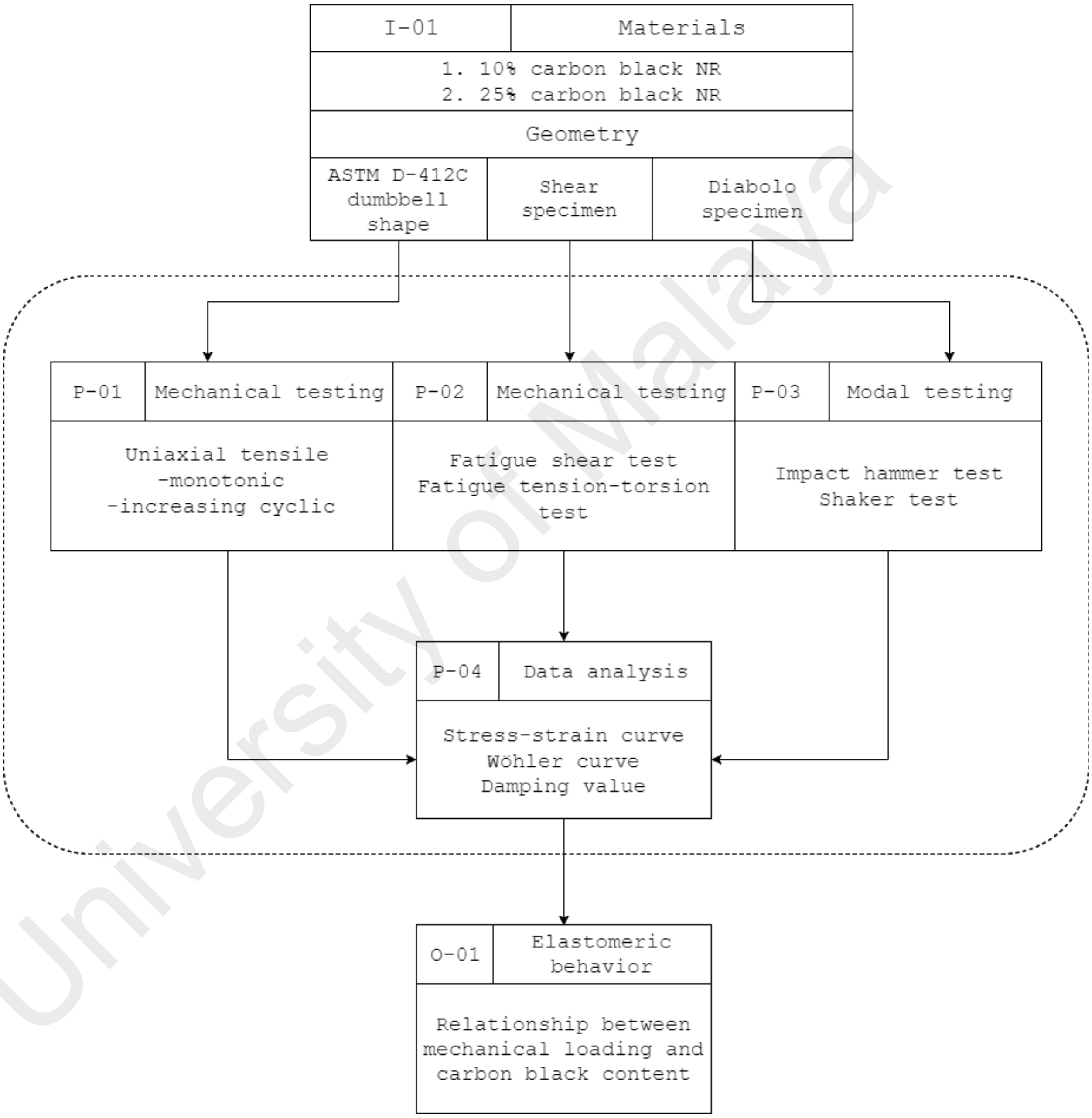

Fig. 3.1. Methodology of research. Note: I for input, P for process, O for output.

3.1 Experimental program

Three mechanical testing will be conducted for collecting experimental database. Experimental specimens and testing machines will be introduced in this section.

3.1.1 Materials and specimen

The materials used throughout the experimental work, natural rubber (NR) are purchased from MAKA Engineering Sdn. Bhd., Malaysia. Two types of natural rubber content are used, with 10wt% carbon black and 25wt% carbon black. In order to carry out different experimental testing, specimens with three geometries are used: dumbbell specimen, shear specimen and diabolo-shaped specimen. The dimension of each specimen are as shown below.

3.1.1 (a) Static uniaxial specimen

Dumbbell specimens of ASTM standard D-412C with thickness of 2 mm are used to conduct static uniaxial testing. The detail of the dimension (in mm) of dumbbell specimen is provided in figure below.

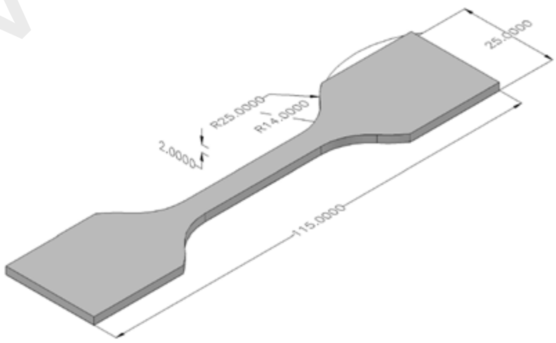

Fig. 3.2. Dumbbell specimen geometry

Two batches of specimens with 10wt% and 25wt% carbon black content are used to study the mechanical behavior under static loading.

3.1.1 (b)   Shear specimen

A simple version of shear specimen is used in the experiment to illustrate the performance of SRD in application (see Figure 3.3. Dimensions are in mm. This made up of sandwiched layer of two rubber part and three metal plates. Suitable adjustment is made in order to be fixed on the fatigue machine.

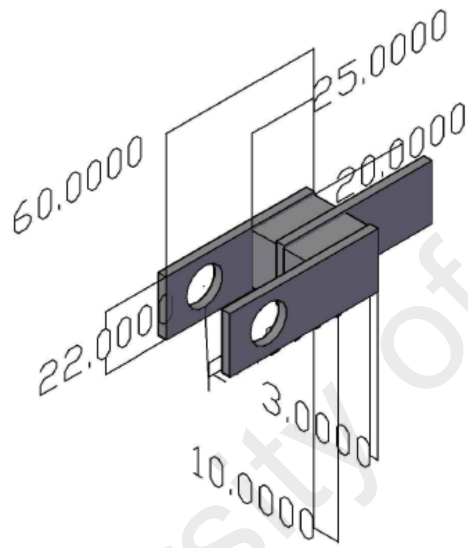

Fig. 3.3. Shear specimen

3.1.1 (c)   Diabolo-shaped specimen

Diabolo-shaped specimen is designed by referring to Lectez et al. (2013) which compatible to the tensile-torsion machine. The specimen is made up of metallic and elastomeric part. Metallic part is attached onto both ends of the elastomeric part as the holder to the machine. Details of the specimen can be refered in Figure 3.4.

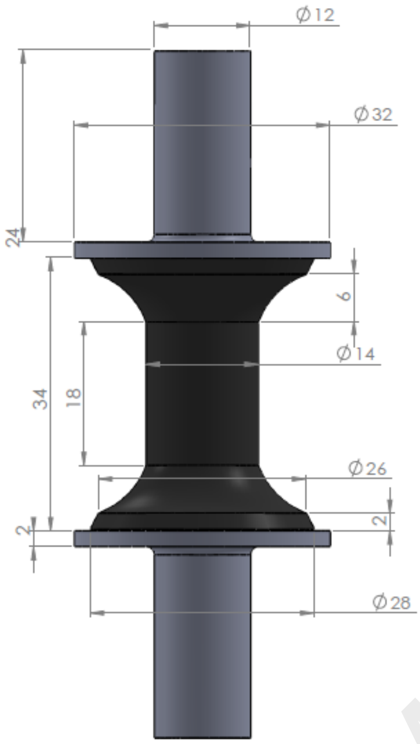

Fig. 3.4. Diabolo shaped specimen (dimensions in mm)

3.1.2 Mechanical test

3.1.2 (a) Uniaxial test

The investigation of elastomeric response is started with static uniaxial test to understand the macroscopic response of the rubber. ASTM D-412C rubber specimen is tested with INSTRON uniaxial test machine having 10kN load cell in room temperature. Data is generated for further investigation.

Two types of mechanical tests are conducted as shown below:

1. Monotonic uniaxial tensile test

   Specimens are subjected to an increasing monotonic tensile load up to fracture.

2. Cyclic tensile test with increasing maximum strain up to 6 cycles.

The profile of the mechanical testing is shown in Figure 3.7 for better illustration.

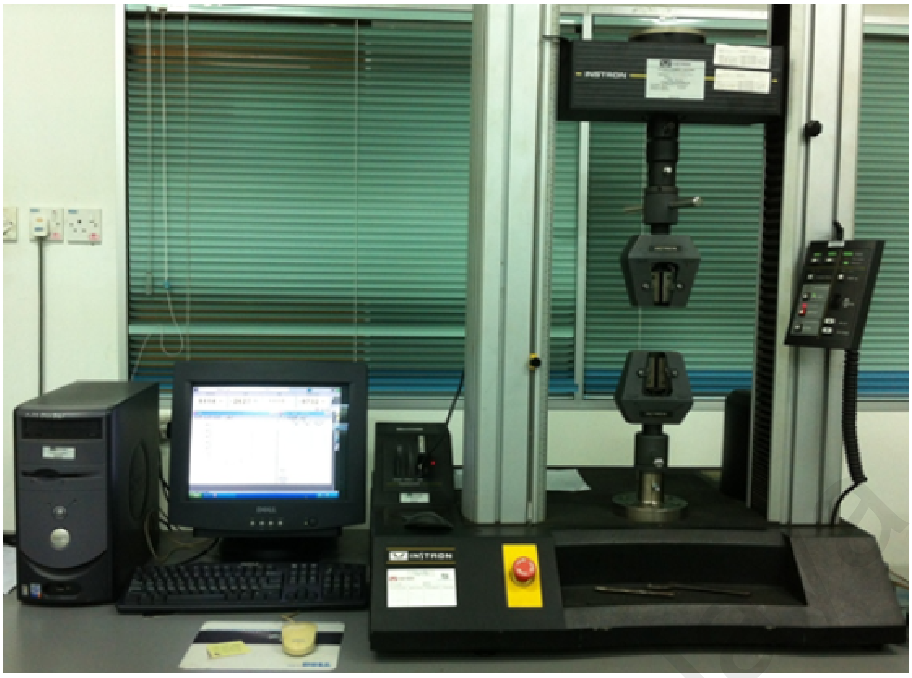

Fig. 3.5. INSTRON uniaxial test machine

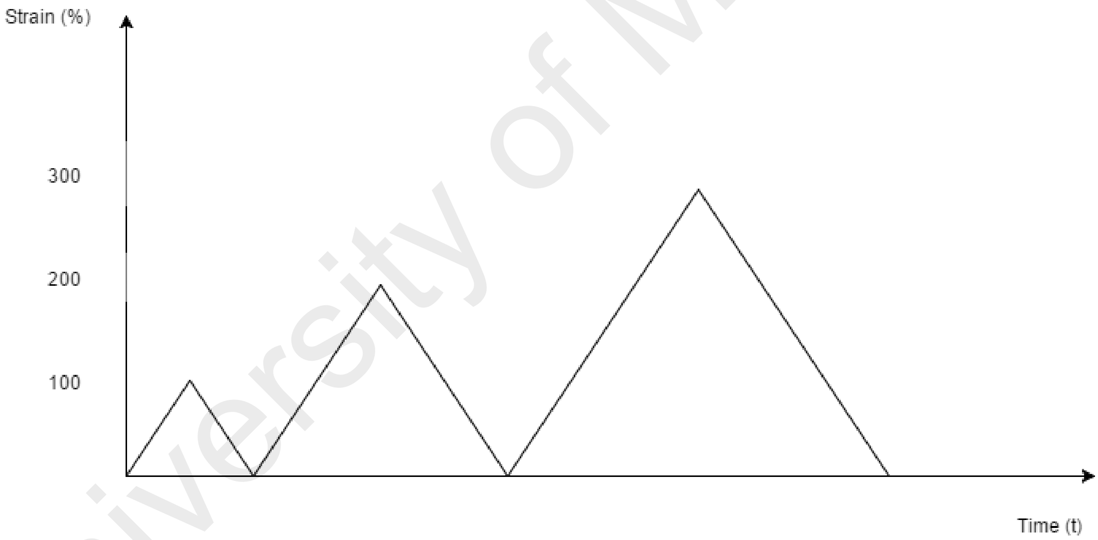

Fig. 3.6. Cyclic tensile test with increasing maximum strain

3.1.2 (b) Cyclic shear test

Fatigue shear test is conducted via SHIMADZU 4830 fatigue testing machine with 5kN load cell. The test is preset to sinusoidal displacement with frequency and displacement loading accordingly. Five level of loading conditions is applied onto the shear specimens with 10wt% and 25wt% respectively. Observation on 1mm crack, 2mm crack and complete failure is done to note the number of cycle when the crack appreared. The test is stopped at 1 million cycles if no crack is observed on the specimen.

Five loading conditions will be applied on the shear specimens as shown in table below. The range of imposed displacement is between 2 to 10mm, which equivalent to the maximum stretch from 1.22 to 2.62. Frequency applied is from 0.5Hz for the highest displacement to 2Hz for the lowest displacement. The experiments are conducted in room temperature.

Fig. 3.1. Mechanical loading conditions for shear test

Test	Maximum Displacement (mm)	Frequency (Hz)
1	2	2
2	4	1
3	6	1
4	8	0.5
5	10	0.5

Using $\boldsymbol{e}_1, \boldsymbol{e}_2, \boldsymbol{e}_3$ cartesian coordinate system, the deformation gradient tensor for simple shear loading is given by Green and Adkins (1960):

$$F = \begin{bmatrix} 1 & \gamma & 0 \\ 0 & 1 & 0 \\ 0 & 0 & 1 \end{bmatrix} \tag{3.1}$$

and the corresponding left Cauchy-Green strain tensor B has the following form:

$$B = \begin{bmatrix} 1+\gamma^2 & \gamma & 0 \\ \gamma & 1 & 0 \\ 0 & 0 & 1 \end{bmatrix} \tag{3.2}$$

γ is given by:

$$\gamma = \frac{u}{h} \tag{3.3}$$

where u is the displacement while h = 10mm is the specimen thickness. It can be shown that the three principal stretches of the above tensor are:

$$\lambda_1 = \left[\left(1 - \frac{\lambda^2}{2}\right) + \frac{\lambda}{2}\sqrt{\lambda^2 - 4}\right]^{\frac{1}{2}} \tag{3.4}$$

$$\lambda_2 = \left[\left(1 - \frac{\lambda^2}{2}\right) - \frac{\lambda}{2}\sqrt{\lambda^2 - 4}\right]^{\frac{1}{2}} \tag{3.5}$$

$$\lambda_3 = 1 \tag{3.6}$$

For construction of Wöhler curve, λ_1 will be taken into account as the maximum principal stretch.

Under simple shear, for Neo-Hookean hyperelastic materials, the corresponding strain energy density W is given by

$$W = C(I_1 - 3) \tag{3.7}$$

where $I_1 = \gamma^2 + 3$

In Equation 3.7, C is a material parameter which can be related to the shear modulus. It can be obtained by fitting the uniaxial tensile test data.

3.1.2 (c)   Combined cyclic tension-torsion test

The following experimental work is conducted at Ecole Centrale de Nantes, France. Multiaxial mechanical testing is performed by using the machine INSTRON E10000. Simultaneous tensile -torsion force can be applied onto the specimen until it reaches the fracture limit. The fatigue test was conducted in room temperature 23°C. End of life of the specimen is defined as 30% reduction in force with reference of 1000th cycle after initiated the test. The test is done by displacement-controlled with the loading conditions as shown in table below:

Fig. 3.2. Mechanical loading conditions for tension-torsion test

Test	Maximum axial displacement (mm)	Angle of torsion (degree)	λ	τ	Frequency (Hz)
1	8.974	50.7	1.54	0.049	4
2	11.538	65.1	1.69	0.063	3.5
3	15.384	86.82	1.91	0.084	2
4	23.076	130.22	2.36	0.126	1.5

Using $\boldsymbol{e}_1, \boldsymbol{e}_2, \boldsymbol{e}_3$ cylindrical coordinate system, the deformation gradient tensor for combined tension-torsion loading is given by Green and Adkins (1960):

$$F = \begin{bmatrix} \frac{1}{\sqrt{\lambda}} & 0 & 0 \\ 0 & \frac{1}{\sqrt{\lambda}} & 0 \\ 0 & \tau r & \lambda \end{bmatrix} \tag{3.8}$$

whereas Cauchy-Green strain tensor B is:

$$B = \begin{bmatrix} \frac{1}{\lambda} & 0 & 0 \\ 0 & \frac{1}{\lambda} + \frac{\tau^2 R^2}{\lambda} & \sqrt{\lambda}\tau R \\ 0 & \sqrt{\lambda}\tau R & \lambda^2 \end{bmatrix} \tag{3.9}$$

where R is the radius, λ is the stretch and τ is the twist per unit of initial length. It can be shown that the three principal stretches of the above tensor are:

$$\lambda_1 = \left[\frac{1}{2} \left(\lambda^2 + \frac{1+\tau^2 R^2}{\lambda} + \sqrt{\left(\lambda^2 + \frac{1+\tau^2 R^2}{\lambda} \right)^2 - 4\lambda} \right) \right]^{\frac{1}{2}} \tag{3.10}$$

$$\lambda_2 = \left[\frac{1}{2} \left(\lambda^2 + \frac{1+\tau^2 R^2}{\lambda} - \sqrt{\left(\lambda^2 + \frac{1+\tau^2 R^2}{\lambda} \right)^2 - 4\lambda} \right) \right]^{\frac{1}{2}} \tag{3.11}$$

$$\lambda_3 = \frac{1}{\sqrt{\lambda}} \tag{3.12}$$

For construction of Wöhler curve, λ_1 will be taken into account as the maximum principal stretch.

Under combined tension-torsion, for Neo-Hookean hyperelastic materials, the corresponding strain energy density W is given by:

$$W = C(I_1 - 3) \tag{3.13}$$

where $I_1 = \lambda^2 + \frac{2+\tau^2 R^2}{\lambda}$

In Equation 3.13, C is a material parameter which can be related to shear modulus. It can be obtained by fitting the uniaxial tensile test data.

3.1.2 (d) Vibration test

Apart from the rubber component, sliding rubber damper device is further tested. Since its potential application will undergo vibration generated from earthquake and wind motion, a simulation test is needed to understand its performance.

Vibration test was conducted on structural frame with 10wt% and 25wt% carbon black sliding rubber damper device to investigate the effectiveness of rubber damper on sliding rubber damper.

Sliding rubber damper device during application is prone to vibration generated from earthquake and wind motion. The dynamic characteristics of a structure can be determined using modal analysis (Trethewey & Cafeo, 1992; Irvine, 2000). In order to understand the performance of SRD a structure model is constructed to conduct the test. Two types of modal analysis are carried out, firstly the impact hammer modal testing and followed by shaker modal testing. SRD with 10wt% carbon black and 25wt% carbon black are attached onto the structure frame as shown in Figure 3.7. In the first test, the structure is knocked for five times using a hammer connected with sensor and load cell. The vibration behaviour is recorded in the system. The same process is repeated on each points of the structure.

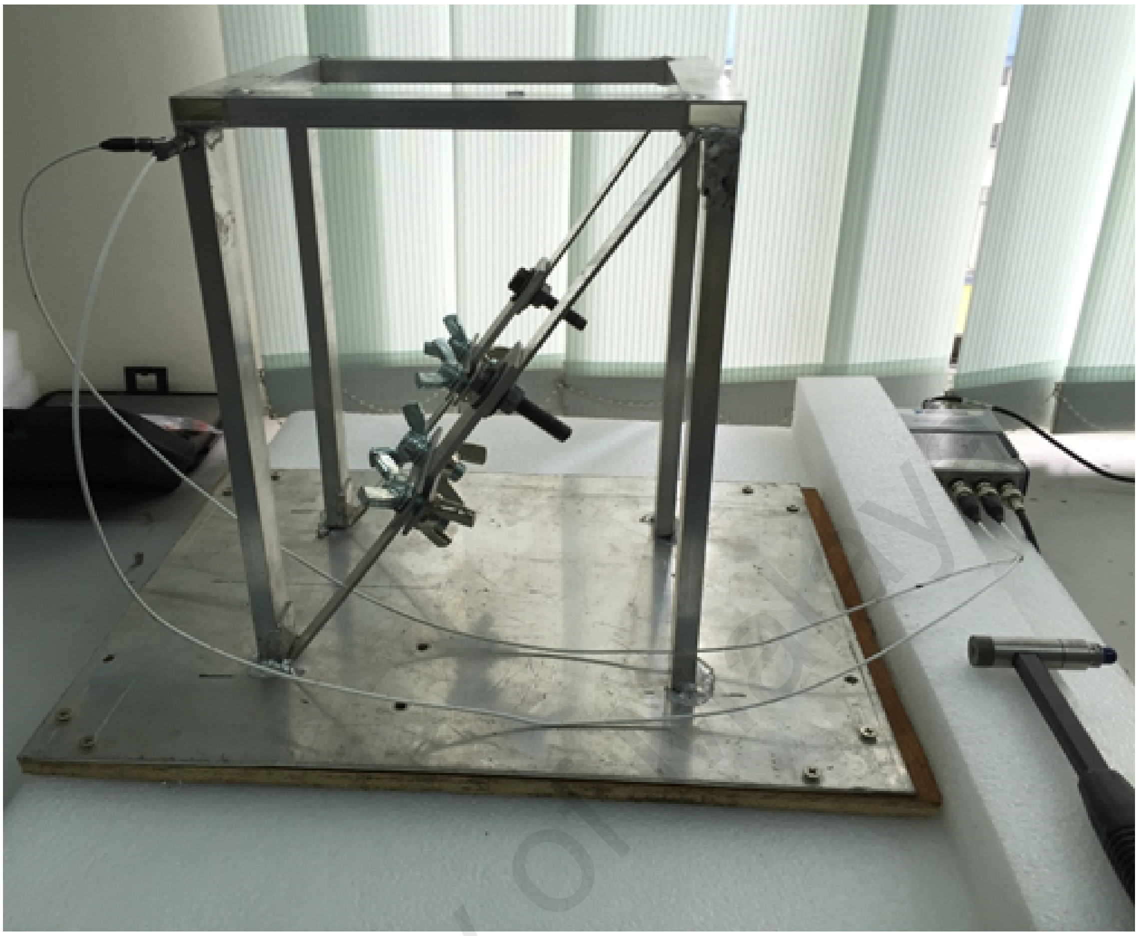

Fig. 3.7. Impact hammer test setup.

The shaker test is set up by attaching the shaker onto the structure frame as shown in Figure 3.8. Based on the impact hammer testing, the natural frequency of the structure is identified. The shaker was initiated at a point with the particular natural frequency of the structure to determine the decay rate.

3.2 Design of new damper system

Recent earthquake phenomenon has occurred in neighbouring countries of Malaysia. Having high chances that earthquake vibration can be transmitted to the surrounding countries, it is important to ensure that the buildings in Malaysia are equipped with earthquake energy dissipation device.

Rubber is extensively used in various industry such as automobile and aerospace. The efficiency of rubber as a damper is inevitable. In civil engineering, it is well known

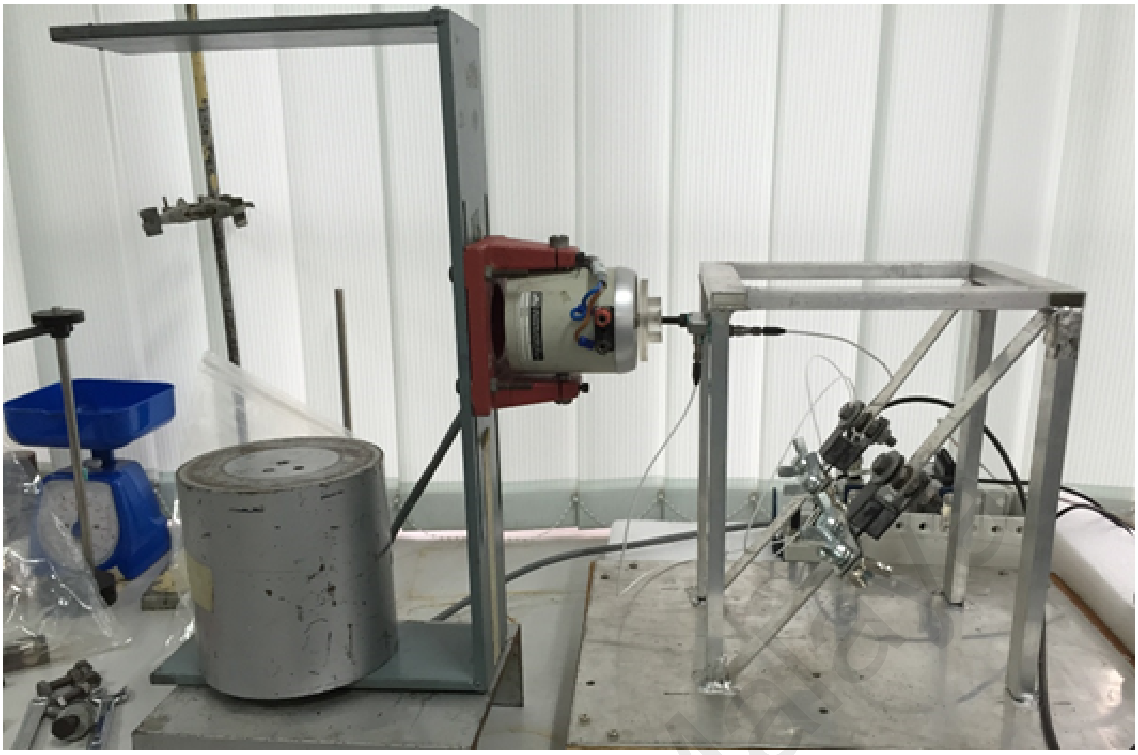

Fig. 3.8. Shaker test setup.

that rubber is used in structural energy dissipation application. There are various structural control system available currently which focuses in the earthquake high risk zone. Active, semi-active and hybrid systems require high technical skill and good maintenance to be implemented in structure. Passive system, however, is a much simple alternative in terms of production and maintenance.

Base isolator is a well-known passive system implemented to dissipate earthquake vibration. However it is not suitable for existing structure as the implementation should be done during the construction. Inspired by the working principle of base isolator, a new damper device is to be proposed which fulfill the criteria as stated below:

- Easy installation
- Good damping performance
- Low maintenance cost

CHAPTER 4: RESULTS AND DISCUSSION

This chapter presents the experimental results obtained from the experimental works as mentioned in the previous chapter. The first part will be explaining the response of elastomer under uniaxial and multiaxial cyclic mechanical loading, followed by the discussion on the results of vibration testing on structure model.

4.1 Mechanical testing results

Three mechanical testings were conducted as mentioned in the previous chapter. Uniaxial mechanical loading was conducted for characterisation. Fatigue testing was conducted both shear and diabolo-shaped specimen to investigate the fatigue behaviour of elastomers under multiaxial cyclic loading.

The later part covers the vibration testing results of structure model. The effect of structure frame with and without damper device will be discussed.

4.1.1 Monotonic loading

Dumbbell shaped specimens with ASTM D-412-C standard were used in this section with the rubber composition of 10wt% carbon black and 25wt% carbon black. Uniaxial tension up to fracture was conducted. 10wt% carbon black and 25wt% carbon black dumbbell specimens fracture at 800% strain and 650% strain respectively as shown in Figure 4.1.

Elastomer with 25wt% carbon black experienced higher stress as compared to 10wt% carbon black. Higher content of filler results in stiffer material thus higher stress is needed in tensile loading. Microscopically, the local strain experienced in the elastomeric matrix is much higher compared to the strain applied macroscopically. 10wt% carbon black material withstand 150% higher strain than 25wt% carbon black as the stress experienced is comparatively lower. Elastomer with lower filler content is less stiff. Local strain exerted

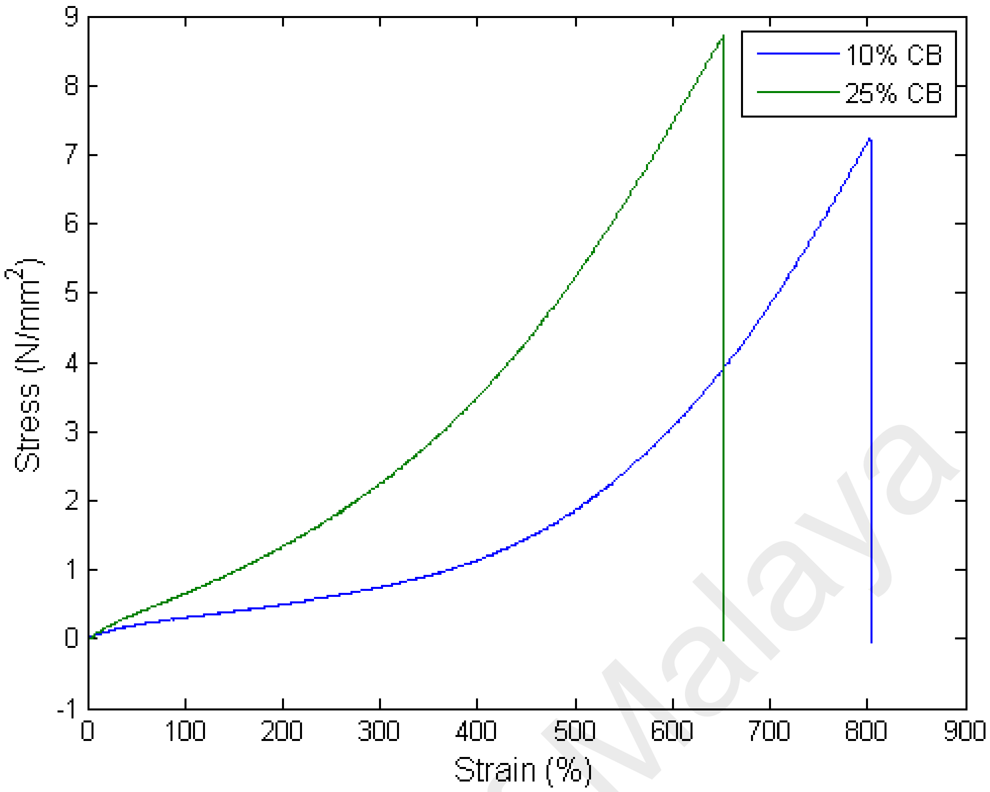

Fig. 4.1. Uniaxial tensile up to fracture for elastomers with 10wt% and 25wt% carbon black content.

due to tensile stretching is lower. Under lower strain condition 10wt% carbon black is able to be stretch further before complete fracture.

Mechanical response of elastomer under increasing cyclic loading is presented as shown in Figure 4.2 and Figure 4.3. The elastomeric specimens were subjected to cyclic tensile with an increment of 100% strain up to 6 cycles. The response of both elastomer with 10wt% and 25wt% carbon black in the first cycle and the 6th cycle of increasing cyclic test can be observed in Figure 4.4 and Figure 4.5. It is significant that 25wt% carbon black elastomer experienced higher stress when subjected to the same amount of strain. Inelastic response were observed in both elastomeric materials. Hysteresis is observed in each cycle of uploading and downloading. Amount of hysteresis is greater at higher strain which can be related with higher heat dissipation. Meanwhile, hysteresis loop for 25wt% carbon black is larger that 10wt% carbon black, indicating 25wt% carbon black experienced higher hysteresis. Carbon black inhibits the movement of rubber matrix during deformation where higher stress is required to deform the rubber component.

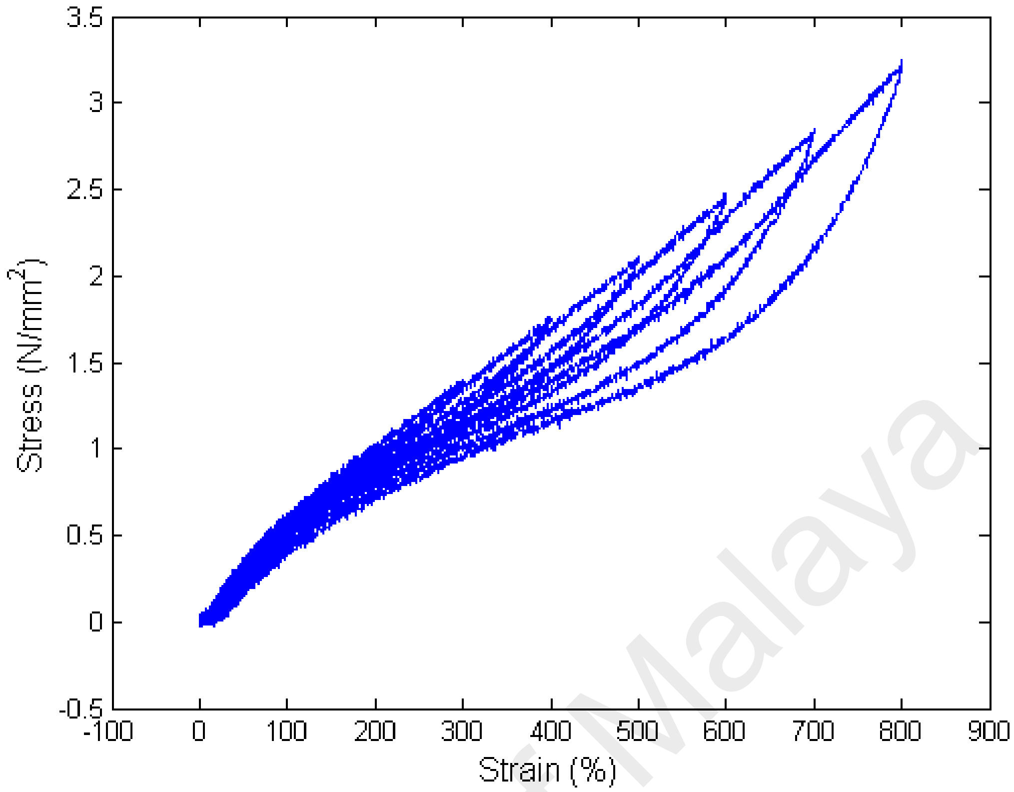

Fig. 4.2. Cyclic tensile test with increasing maximum strain test for 10wt% carbon black

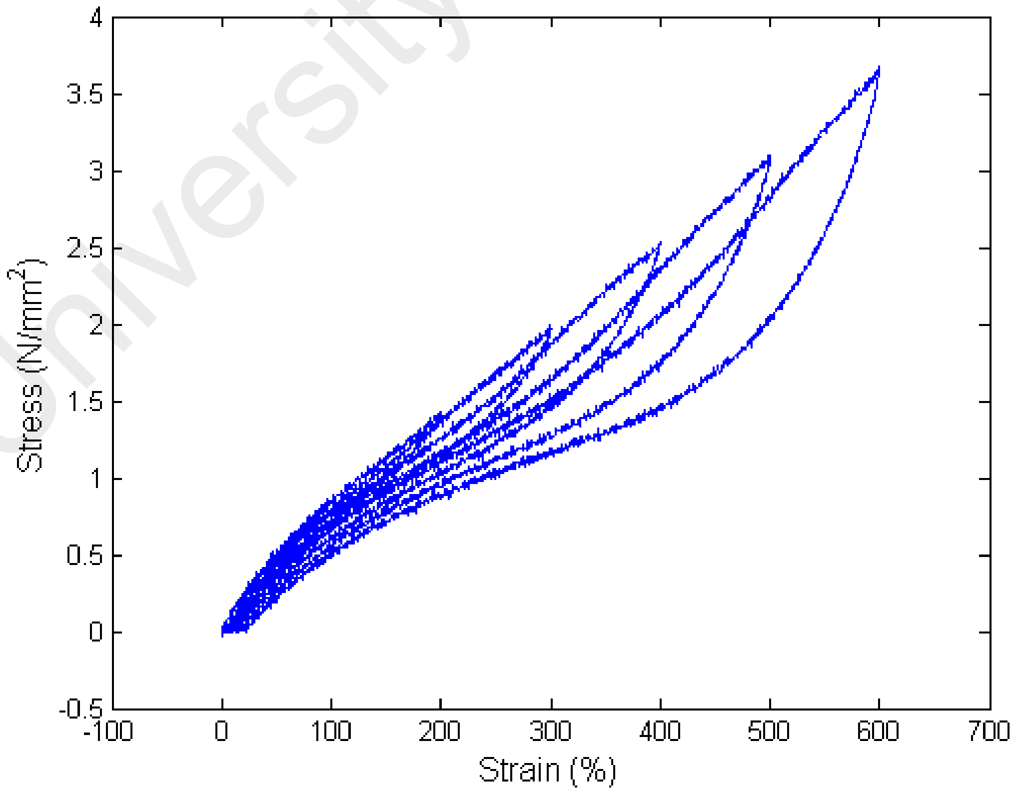

Fig. 4.3. Cyclic tensile test with increasing maximum strain test for 25wt% carbon black

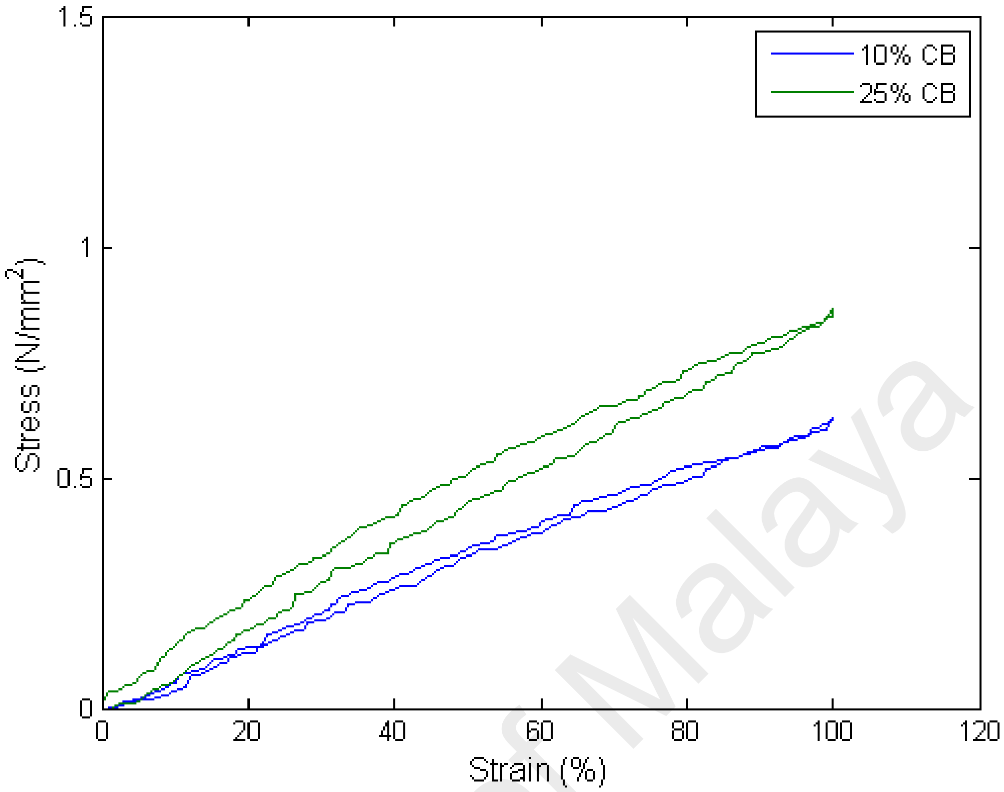

Fig. 4.4. First cycle of increasing cyclic test

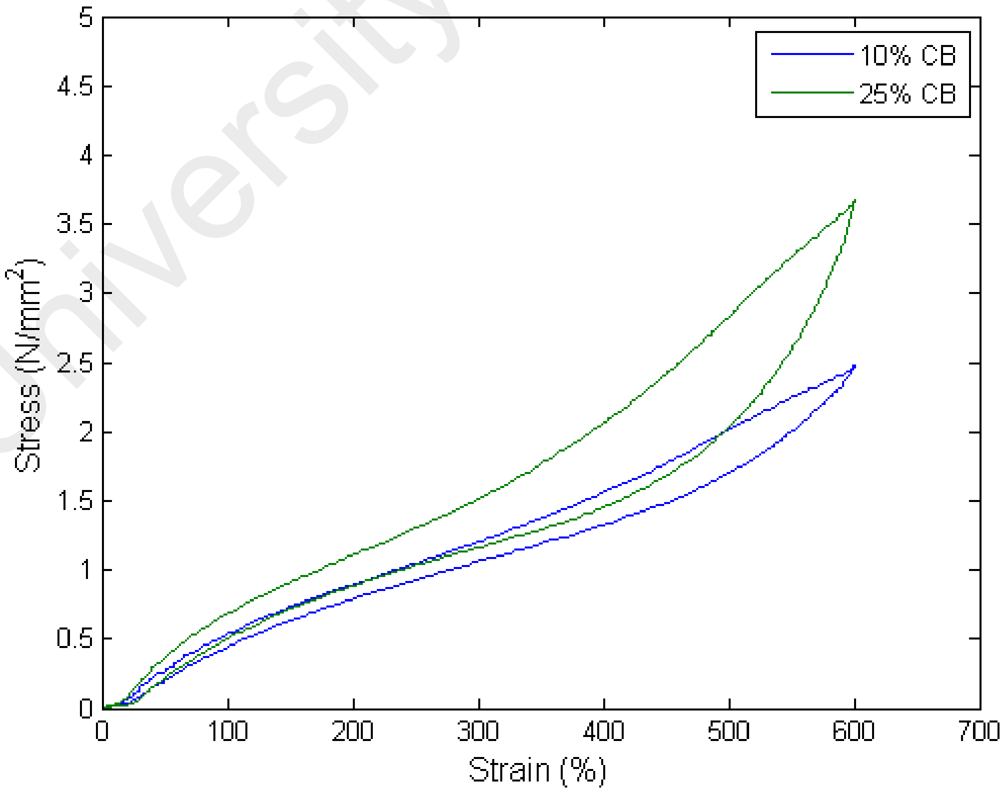

Fig. 4.5. 6th cycle of increasing cyclic test

4.1.2 Fatigue testing

Two fatigue testings were conducted as mentioned in Chapter 3. Firstly, fatigue testing was carried out on specially designed shear specimens. Secondly, combined cyclic tension-torsion was tested on diabolo-shaped specimens. Different geometries were needed to take into consideration when relating local quantities and experimental measurement of tensile and torsion which has been included in Chapter 3.

Figure 4.6 and 4.7 shows the force-number of cycles to failure graph for 10wt% 25wt% shear specimen. The first 100 cycles during the test was not shown as the fatigue machine has not reached the displacement peak set in the system. The force started to stabilized after about 100 cycles after starting the test. The specimen experienced force drop when the sample started to crack or detachment of the metal and rubber part occurred. The specimen will stop when it reaches the maximum number of cycles or failure occur before reaching the maximum number of cycles. For 10wt% carbon black specimens with 8mm and 10mm displacement, it was observed that the force drop at a higher rate compared to the other specimens as the detachment occurred and the tests were terminated. On the other hand, specimens with 2mm, 4mm and 6mm displacement experienced force drop at a slower rate. Detachment did not observed for 2mm, 4mm and 6mm specimens. The end of life of the specimen was defined as 30% drop in force with the reference at 1000th cycle.

The lifetime of the 10wt% specimens were longer than 25wt% under same amount displacement. However it is needed to look into the force exerted on each specimens. Force applied to 25wt% specimens is about double of 10wt%. The lower displacement experienced longer lifetime, which can be seen in specimens with 2mm displacement. Apart from difference in force, the amount of filler may affect the resulting lifetime (Mars & Fatemi, 2004a) which will be discussed in the following part.

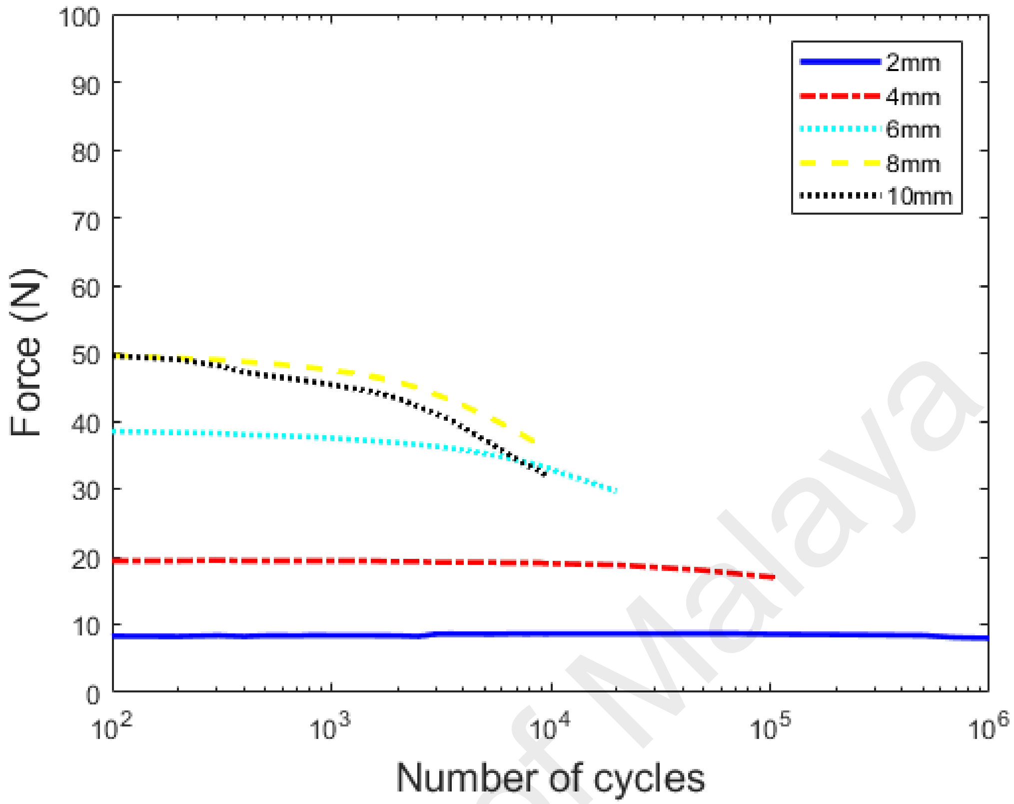

Fig. 4.6. Force vs number of cycles for 10wt% CB cyclic shear.

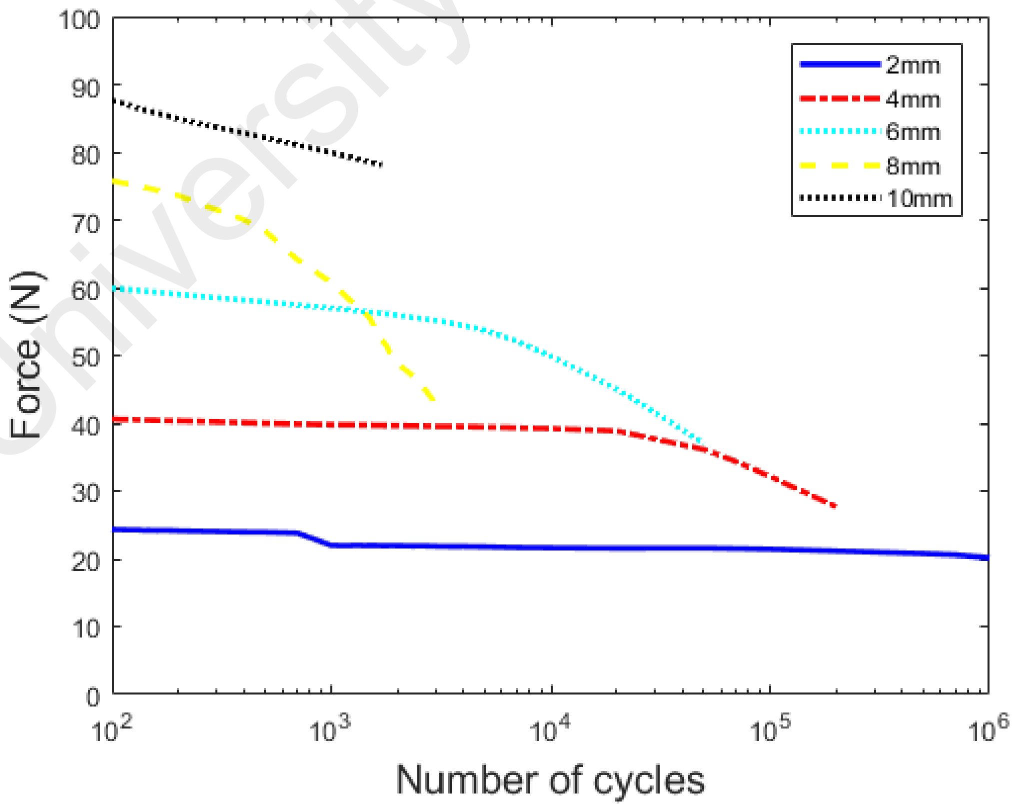

Fig. 4.7. Force vs number of cycles for 25wt% CB cyclic shear.

Different levels of displacement and angle of torsion were applied to diabolo specimens as shown in Table 3.2. The graphs of force-number of cycles for 10wt% and 25wt% diabolo specimens were shown in Figure 4.8 and 4.9. It can be observed that the force experienced was higher for the case of 25wt%. Higher displacement and torsion applied on the specimens resulting shorter lifetime. It is more noticeable for test 3 and test 4 specimens in Figure 4.9 as the force exerted was about 30-40% higher than 10wt% specimens. For lower strech level, the lifetime for both 10wt% and 25wt% specimens were about the same. It can be expected that with the same amount of load applied for both types of specimens, 25wt% may have longer lifetime.

The fatigue results are presented in the form of Wöhler curve. The largest principal stretch, λ_{max} is chosen to be the predictor as cracks tend to propagate on the plane perpendicular to the associated principal direction (Andriyana et al., 2010). The computation of the largest principal stretch will be conducted in two ways as follow:

1. Without explicitly considering carbon black content. For a given imposed loading, the largest principal stretch is computed by using Equations 3.4 and 3.10
2. Explicitly considering carbon black content through the use of strain amplification concept. In this case, the global largest principal stretches given in Equation 3.4 and 3.10 have to be corrected by an amplification factor χ as follow (Guth & Gold, 1938):

$$\lambda_{loc} = \chi(\lambda_{glo} - 1) + 1 \tag{4.1}$$

where λ_{loc} is the local largest principal stretch, λ_{glo} is the global largest principal stretch given in Equations 3.4 and 3.10. Here, the strain amplification factors χ are estimated according to Guth and Gold (Guth & Gold, 1938) and Nielson (Nielsen,

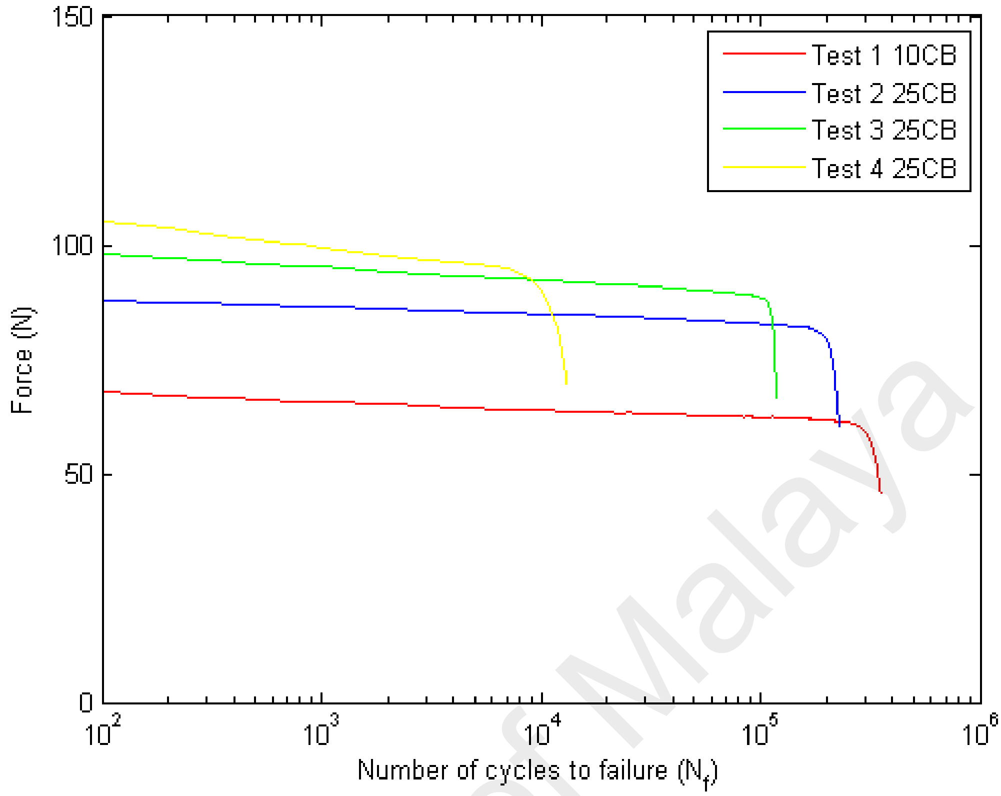

Fig. 4.8. Force vs number of cycles for 10wt% CB combined cyclic tension-torsion.

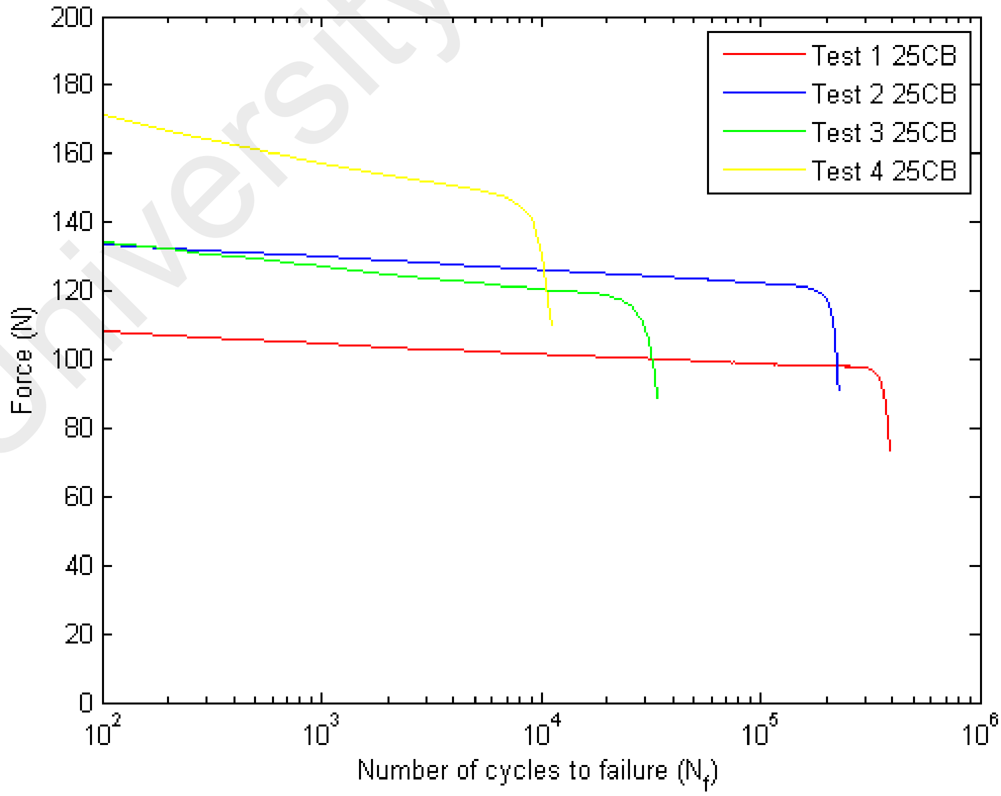

Fig. 4.9. Force vs number of cycles for 25wt% CB combined cyclic tension-torsion.

1966). Their expressions are respectively:

$$\chi_{Guth-Gold} = 1 + 2.5\phi + 14.1\phi^2 \tag{4.2}$$

$$\chi_{Nielson} = \frac{1}{1 - \phi^{1/3}} \tag{4.3}$$

In the above expressions, ϕ is the volume fraction of filler.

Based on the results obtained, Wöhler curve is obtained for two types of elastomeric specimens, subjected to shear and multiaxial tension-torsion deformations. Due to different loading conditions, the graph indicated maximum stretch to number of cycles. Two types of rubber formulations were used, 10wt% carbon black and 25wt% carbon black. According to the graph shown in Figure 4.10, combined cyclic tension-torsion experienced higher maximum principle stretch compared to cyclic shear loading. This highlights the limitation of maximum principal stretch as fatigue prediction as widely known in the literature (Mars & Fatemi, 2002; Roberts & Benzies, 1977). Specimens experienced shorter lifetime when subjected to higher stretch. For 25wt% carbon black specimens, similar trend was observed for both shear and tension-torsion cyclic loading as shown in Figure 4.11. As expected, specimens with lower stretch has longest lifetime. The maximum cycle for both shear and diabolo-shaped specimens were preset at 1 million cycles. Diabolo-shaped specimens breaks before reaching 1 million cycles, while shear specimens reached maximum cycle for only the lowest principle stretch loading condition.

Generally 10wt% carbon black specimens for both shear and diabolo-shaped specimens experienced longer lifetime as compared to 25wt% carbon black specimens as presented in Figure 4.12 and Figure 4.13. Under same amount of stretching, the individual force experienced by each of the rubber content are different, where stiffer material, 25wt% rubber experienced higher stress, and lower for 10wt% rubber. Lower stress experienced by 10wt% rubber resulted longer lifetime.

The effect of strain amplification is shown in Figure 4.14 and Figure 4.15 by considering Guth and Gold strain amplification factor. It can be observed that the maximum principal stretch experienced locally is higher compared to the global stretch. Global stretch which does not takes into account the effect of carbon black do not clearly represents the actual mechanical response experienced by the rubber component. With consideration of strain amplification factor, the presence of carbon black as filler inhibits the stretching of surrounding rubber matrix, resulting higher local stretch. The same scenario can be expected when using Nielson strain amplification theory as presented in Figure 4.16 and Figure 4.17.

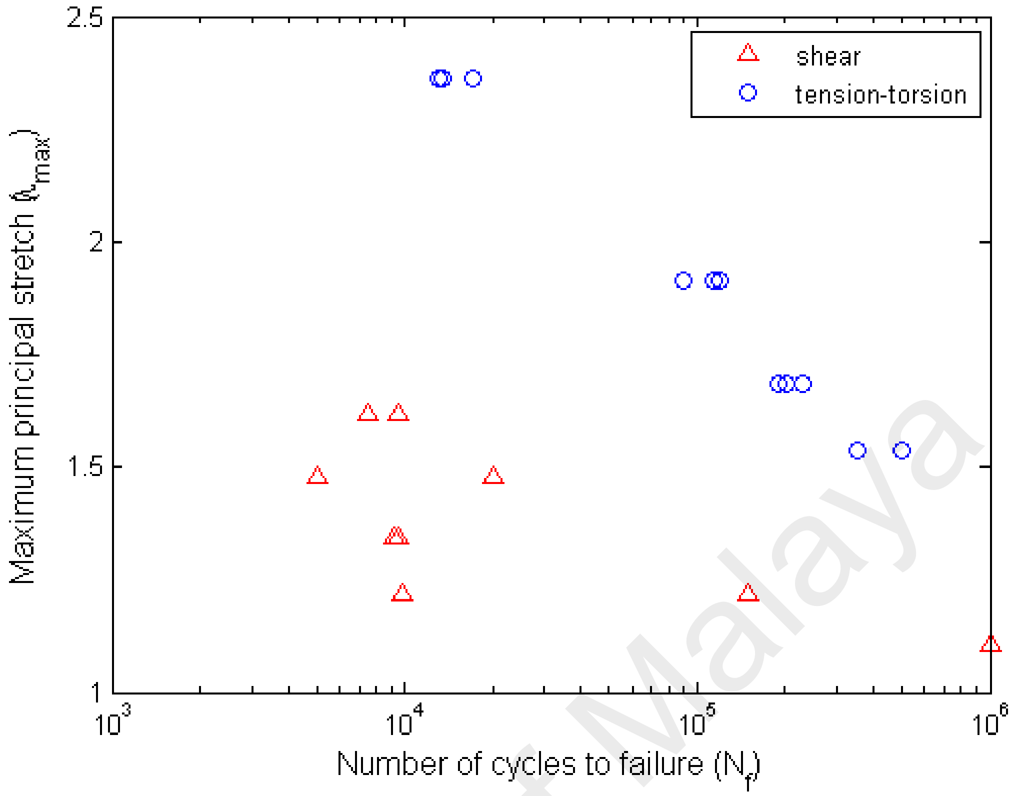

Fig. 4.10. Cyclic shear and combined cyclic tension-torsion test for 10wt% carbon black specimens.

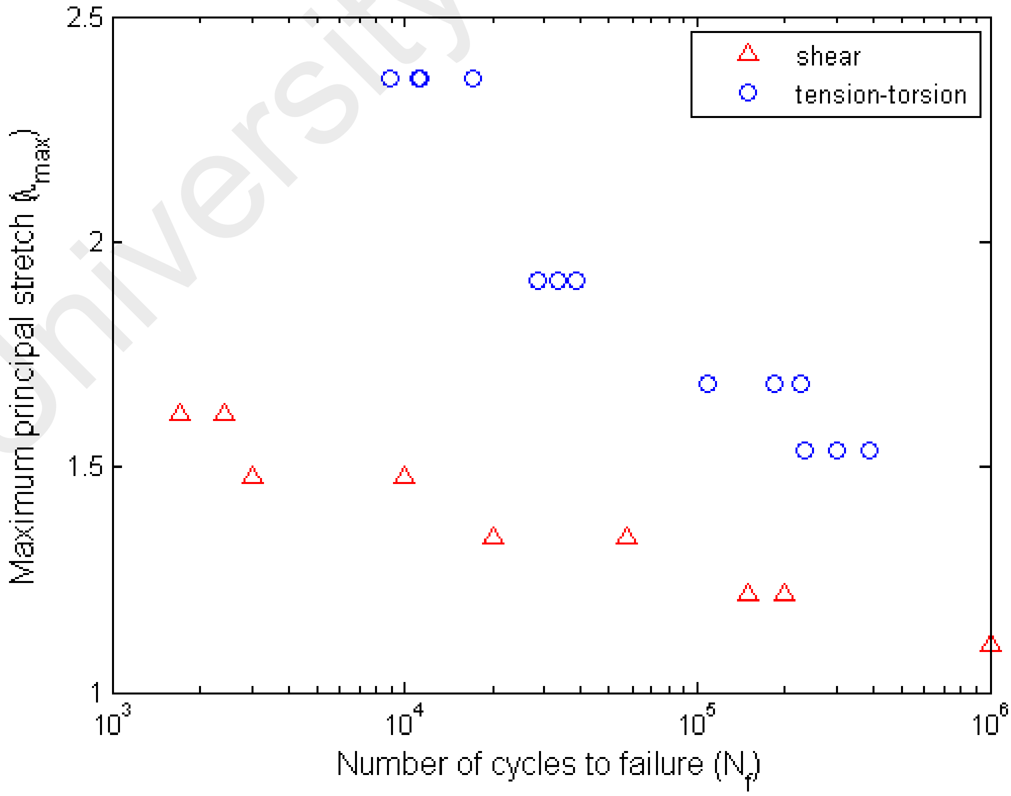

Fig. 4.11. Cyclic shear and combined cyclic tension-torsion test for 25wt% carbon black specimens.

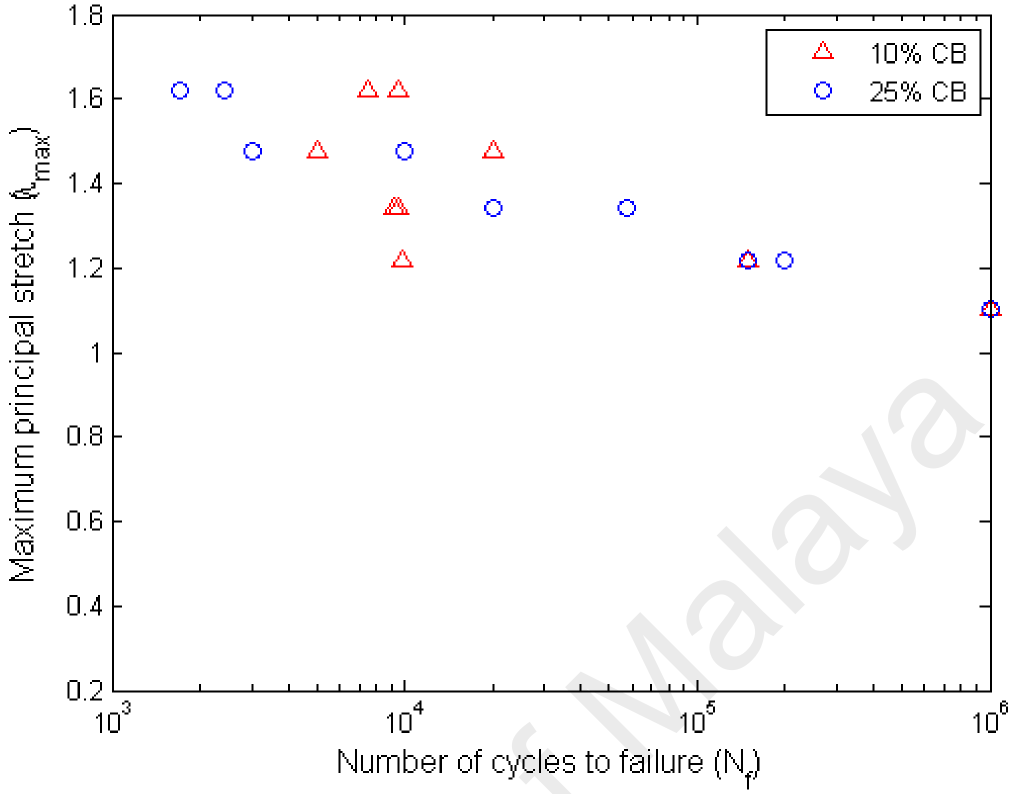

Fig. 4.12. Cyclic shear test for 10wt% and 25wt% carbon black specimens.

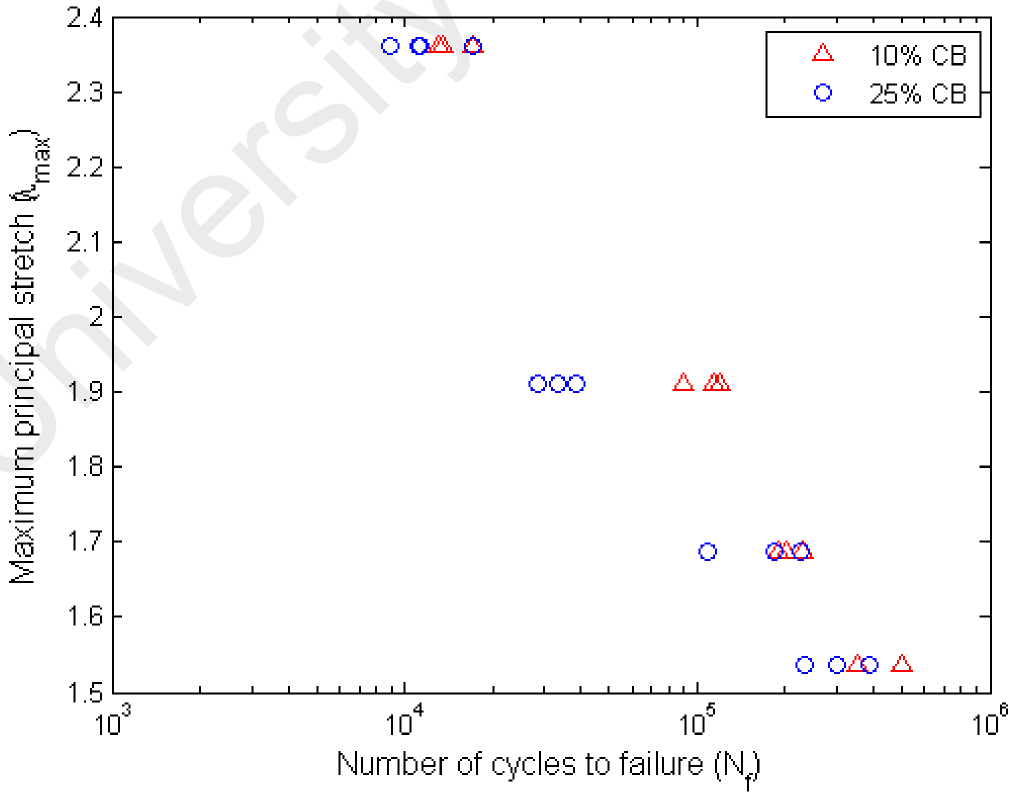

Fig. 4.13. Combined cyclic tension-torsion test for 10wt% and 25wt% carbon black specimens.

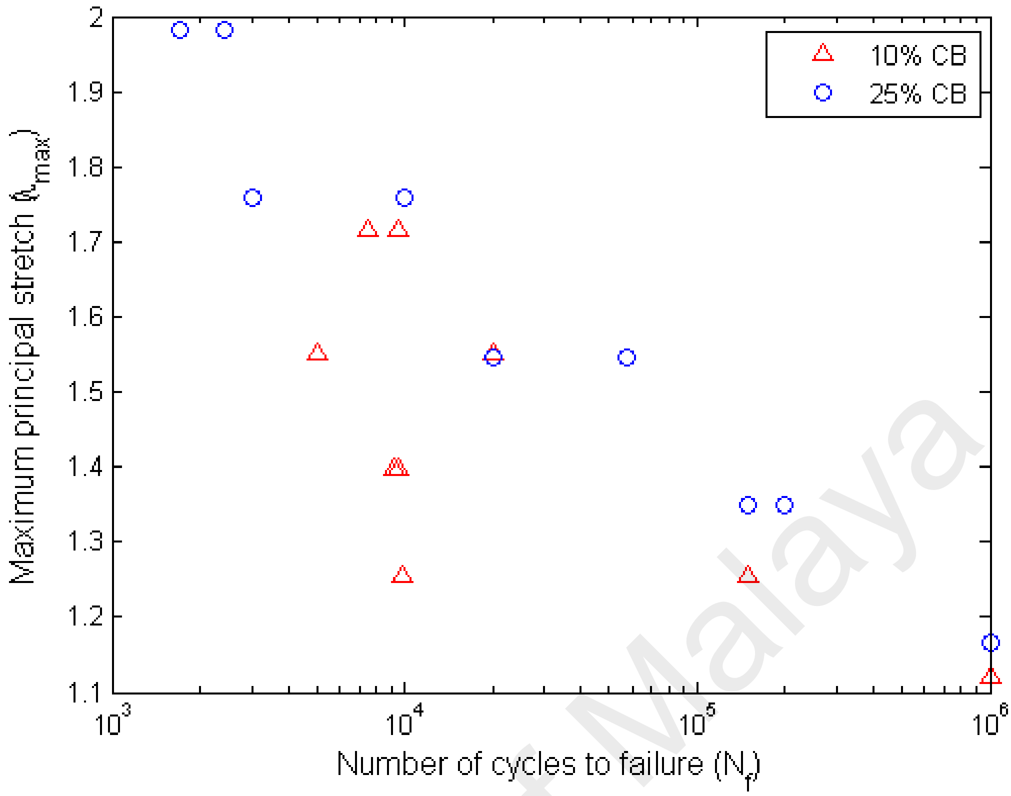

Fig. 4.14. Cyclic shear test for 10wt% and 25wt% carbon black specimens according to Guth and Gold theory.

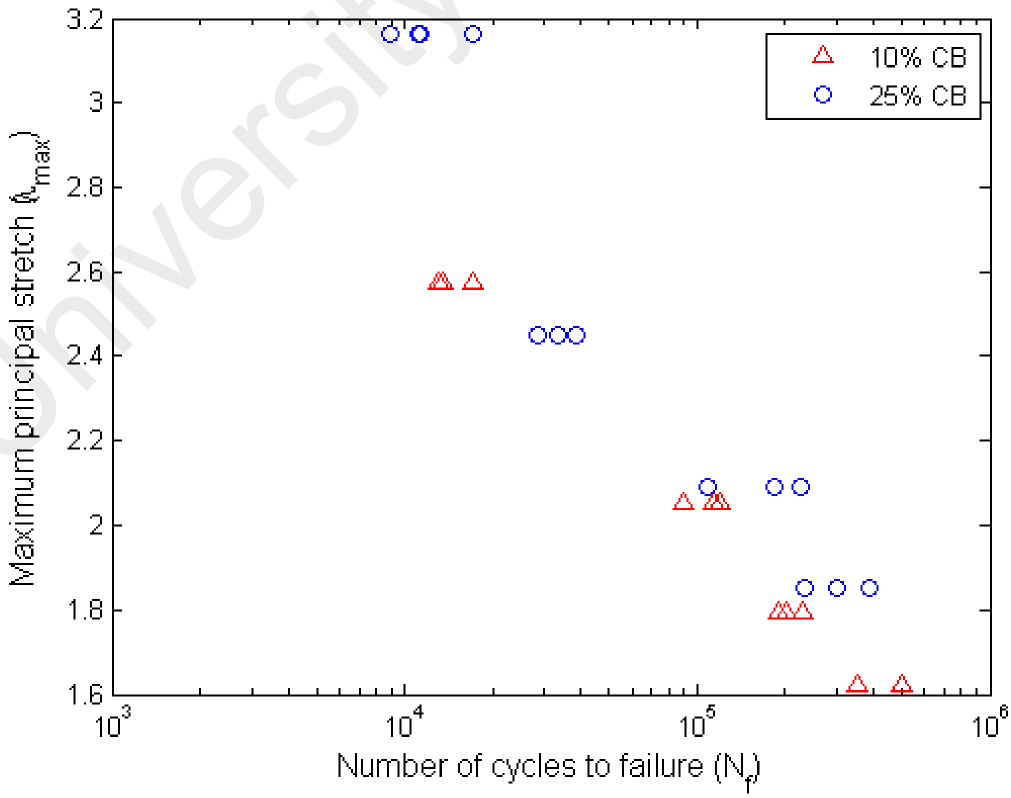

Fig. 4.15. Combined tension-torsion test for 10wt% and 25wt% carbon black specimens according to Guth and Gold theory.

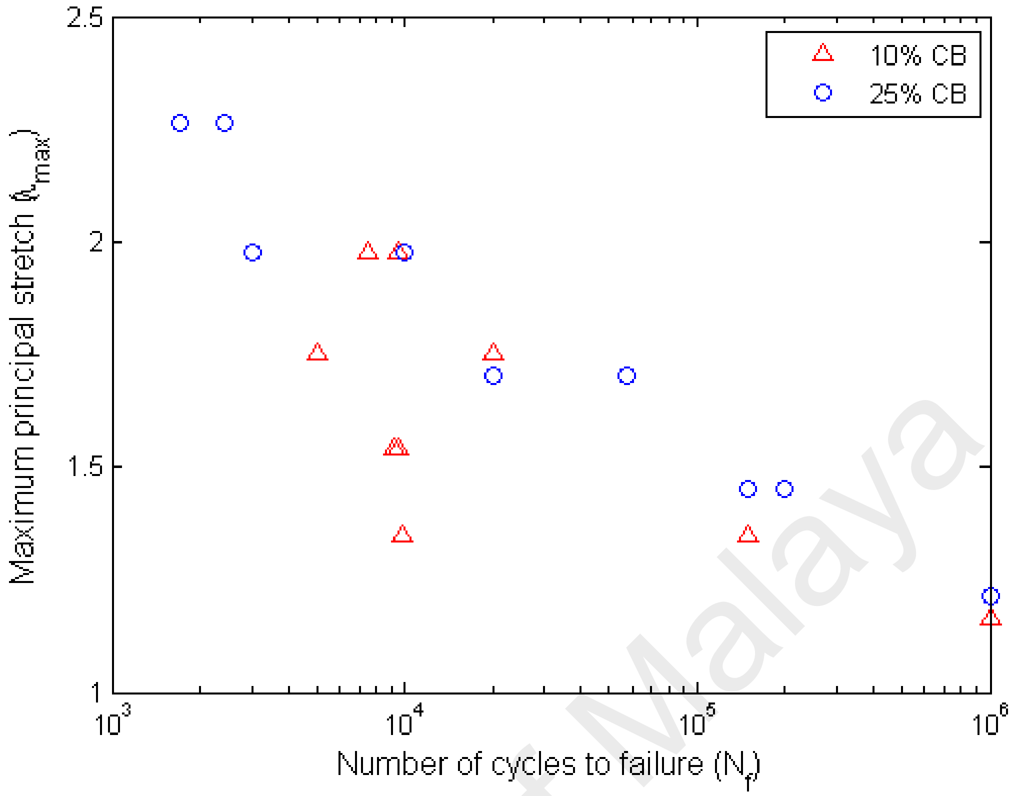

Fig. 4.16. Cyclic shear test for 10wt% and 25wt% carbon black specimens according to Nielsen theory.

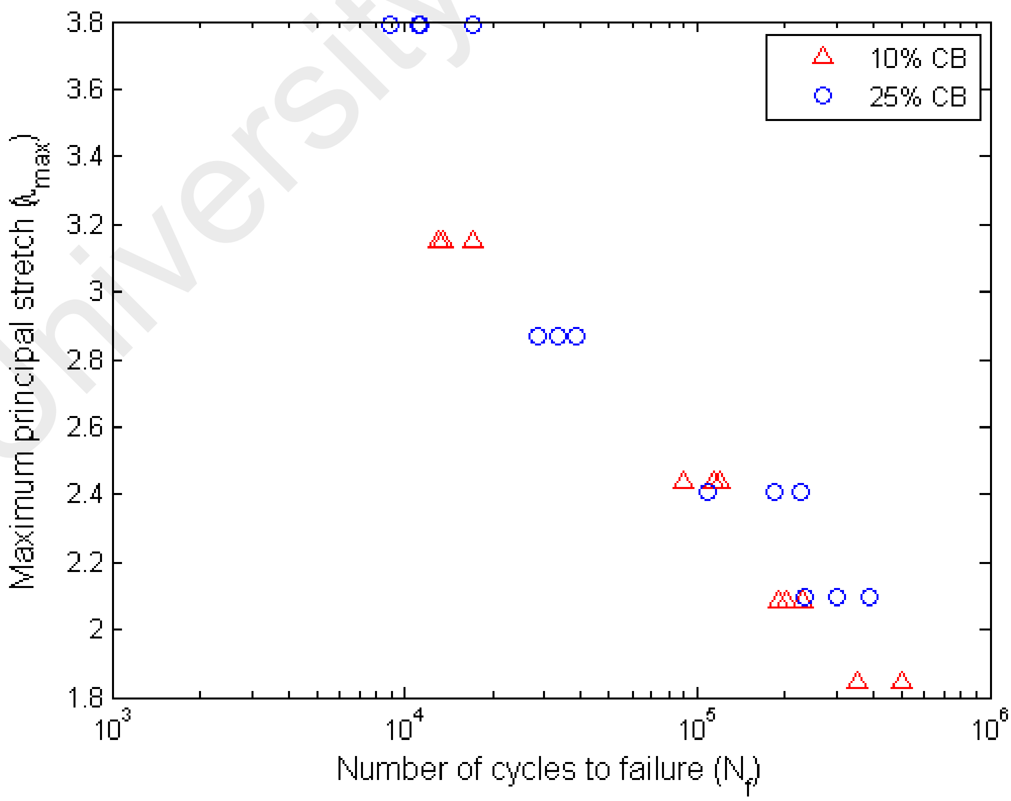

Fig. 4.17. Combined tension-torsion test for 10wt% and 25wt% carbon black specimens according to Nielsen theory.

In addition to largest principal stretch, the strain energy density will be used as the fatigue predictor. Similarly to the largest principal stretch, the computation of strain energy density will be conducted in two ways as follow:

1. Without explicitly considering carbon black content. For a given imposed loading, the strain energy is computed using Equations 3.7and 3.13.

2. Explicitly considering carbon black content through the use of strain amplification concept. In this case, the global strain energy given in Equation 3.7and 3.13 have to be corrected by an amplification factor χ as follow (Qi & Boyce, 2004):

$$W_{loc} = C([I_1]_{loc} - 3) \quad \text{where} \quad [I_1]_{loc} = \chi(I_1 - 3) + 3 \tag{4.4}$$

   where W_{loc} and $[I_1]_{loc}$ are the local strain energy and local first invariant respectively. I_1 is the global first invariant as given in Equations 3.7and 3.13. In Equation 4.4 C=0.16MPa, for 10%CB and C= 0.24MPa for 25%CB. Both are obtained by fitting uniaxial tensile test data as given in Figure 4.1.

Without considering locally the effect of carbon black content as presented in Figure 4.18 and 4.19, the strain energy density for 25wt% specimens are much higher than specimens with 10wt%. In terms of mechanical deformation, specimens experienced higher strain energy density in combined tension-torsion.

The effect of carbon black is prominently seen in Figure 4.20 and Figure 4.21 according to Guth and Gold theory; whereas for Figure 4.22 and Figure 4.23 are based on Nielson's strain amplification factor.

For shear specimens, strain energy density is two times higher for material with higher carbon black content. With consideration of local strain amplification factor, the strain energy density at the initial state was much higher than global.

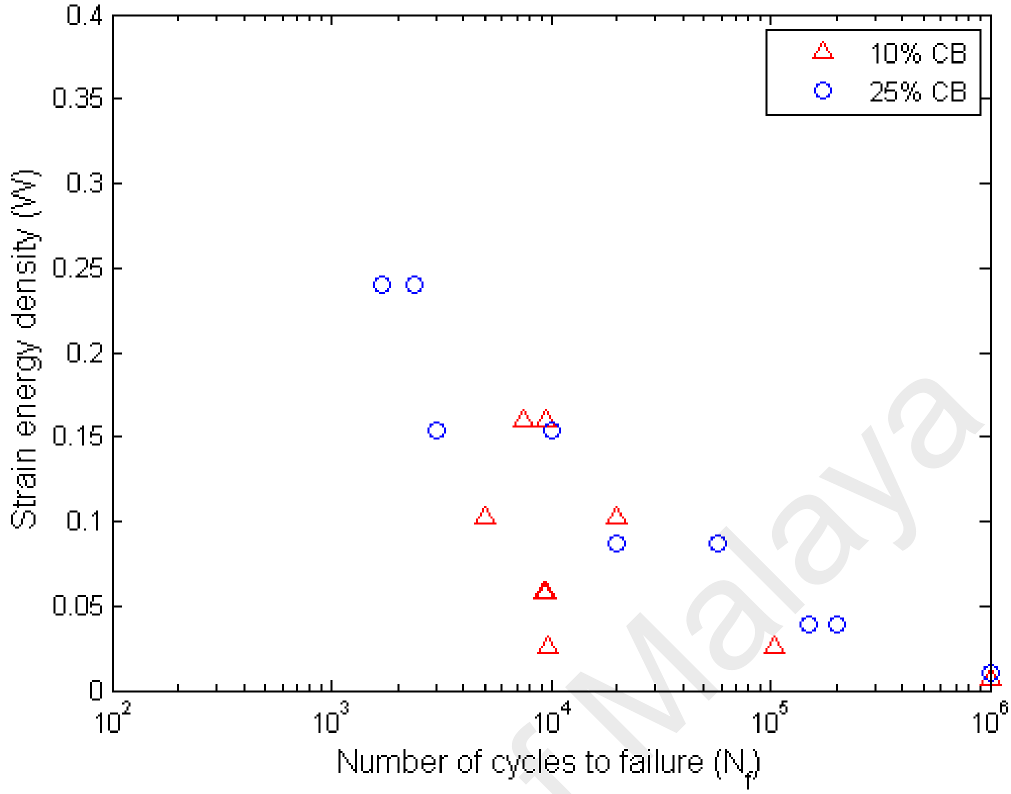

Fig. 4.18. Cyclic shear test for 10wt% and 25wt% carbon black specimens.

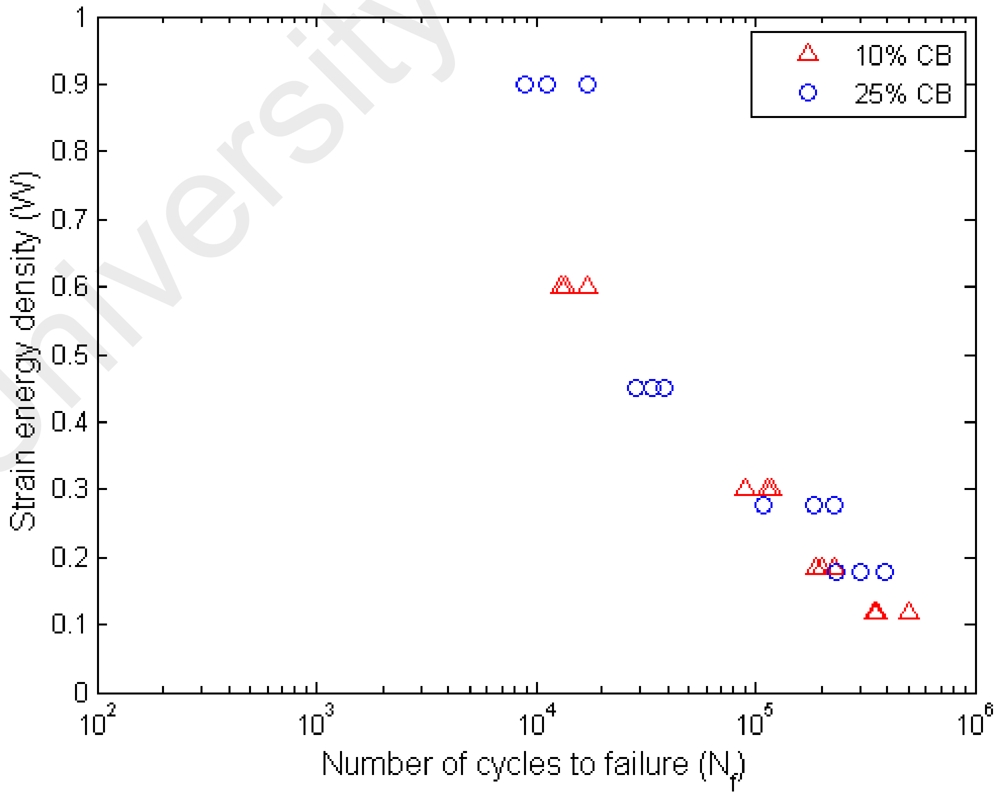

Fig. 4.19. Combined tension-torsion test for 10wt% and 25wt% carbon black specimens.

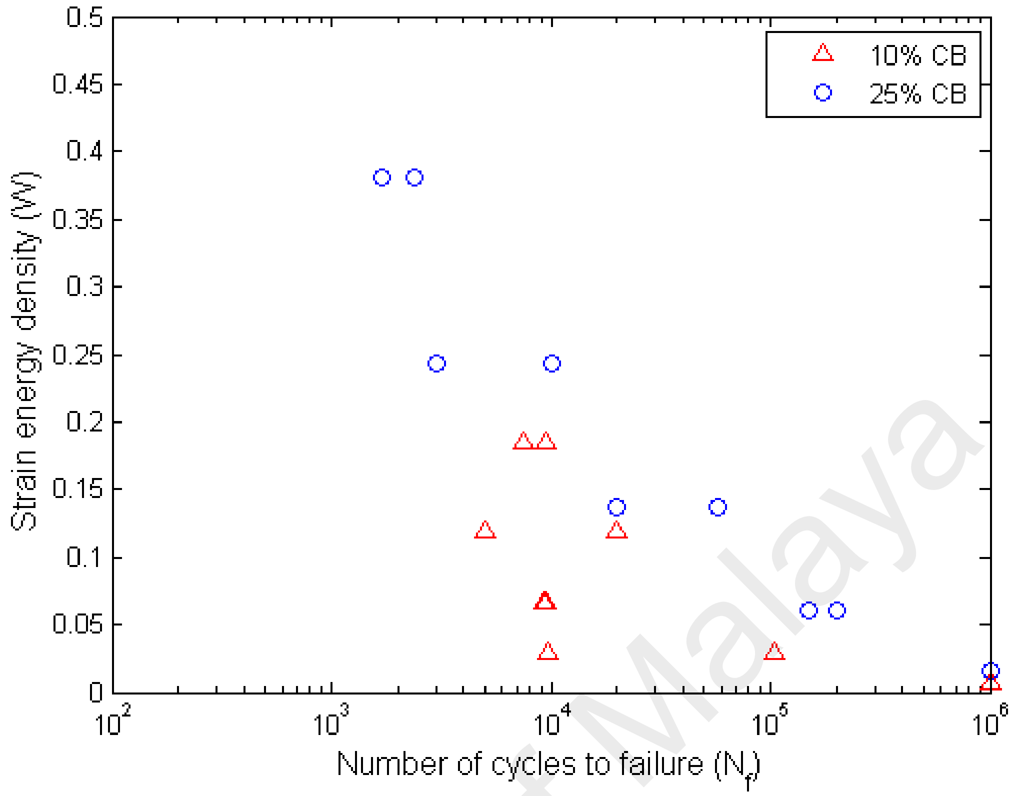

Fig. 4.20. Cyclic shear test for 10wt% and 25wt% carbon black specimens according to Guth and Gold theory.

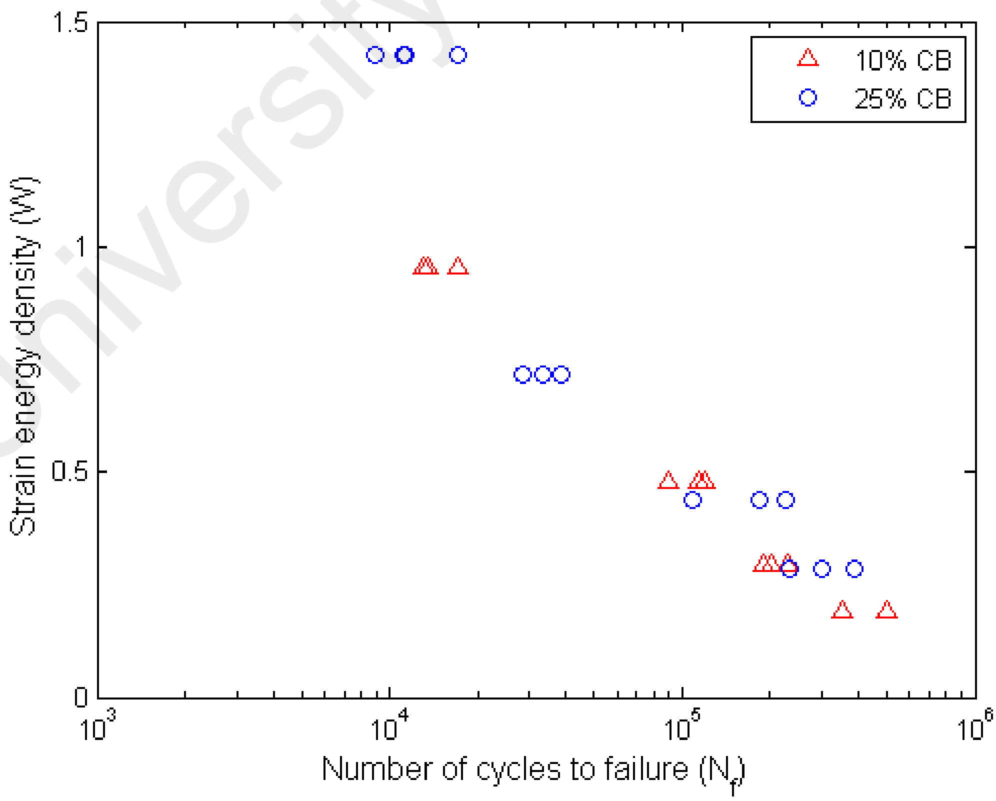

Fig. 4.21. Combined tension-torsion test for 10wt% and 25wt% carbon black specimens according to Guth and Gold theory.

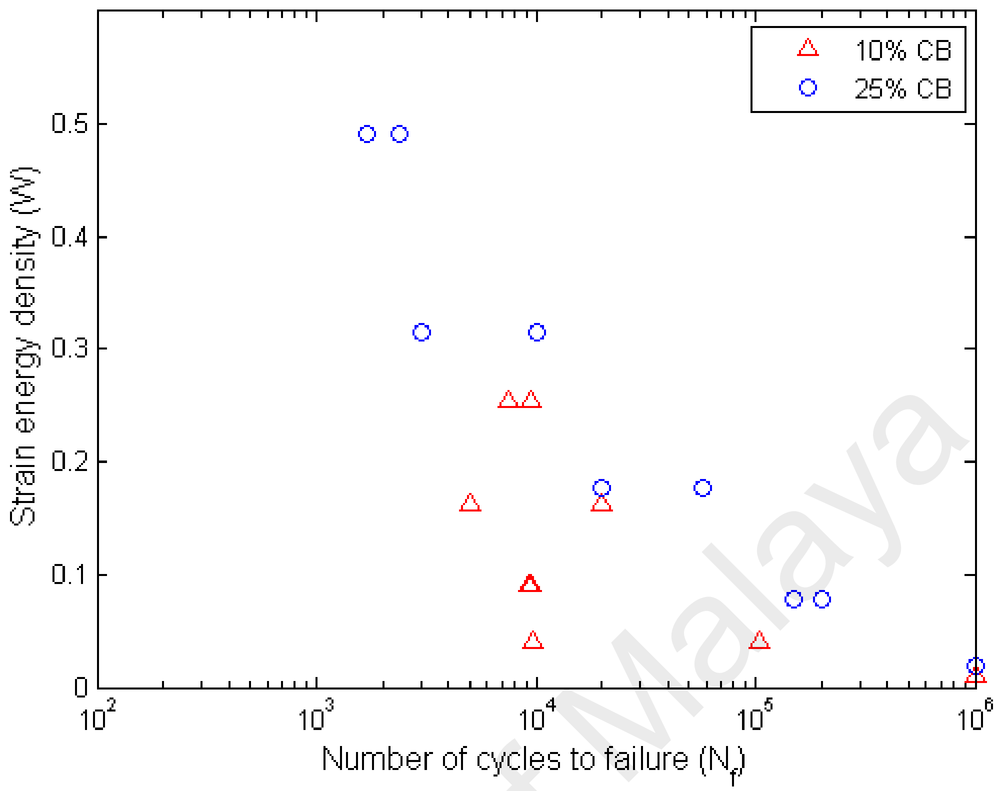

Fig. 4.22. Cyclic shear test for 10wt% and 25wt% carbon black specimens according to Nielsen theory.

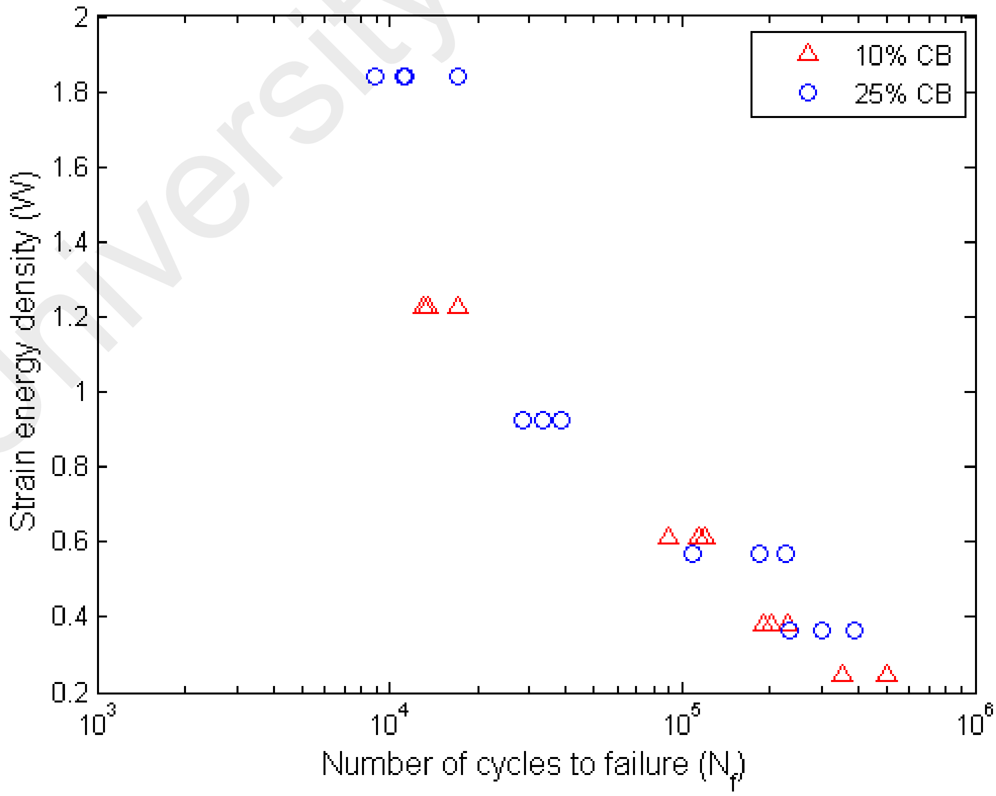

Fig. 4.23. Combined tension-torsion test for 10wt% and 25wt% carbon black specimens according to Nielsen theory.

4.2 Design of new damper system

Passive energy dissipaters are effective in reducing the structural response under vibration loadings. A new passive energy dissipation device for earthquake energy dissipation application was proposed utilizing the elastomeric materials that has been tested in this work. Rubber was chosen to be the mode of energy conversion material due to its low cost and easily available in Malaysia. The working principle of this device is to reduce the effect of vibration generated by earthquake and wind by shear. In order to absorb energy generated by wind and vibration from the ground, it has to be highly elastic, high damping and large elongation at failure. Natural rubber, is one of the commonly used rubber in civil engineering structures. The details of the proposed sliding rubber damper system is presented in Figure 4.24.

In construction, reinforcement of building can be achieved using cross bracing system diagonally for supports. Bracing can increase a building's capability to withstand seismic activity from an earthquake. Bracing is important for an earthquake resistant building as it helps to withstand the structure from collapse. Cross bracing is usually seen with two diagonal supports placed in an X shaped manner experiencing compression and tension forces. Initiated from this idea, a simple device, sliding rubber damper (SRD) is constructed to retrofit current buildings that has no installment of earthquake resistant device.

The structure composed of rubber component and metal plates. Rubber part plays an important role in this system. On the other hand, mild steel is proposed for the supporting material in the system. Strong adhesive between the rubber layers and metal plates will be applied to ensure that no detachment occurs during service. The device can be installed onto the building frame diagonally as shown in Figure 4.25, with the elements as shown in Figure 4.24. Several views of the device is presented to have clearer view of this device as in Figure 4.26, Figure 4.27 and Figure 4.28. The size of the device can be customized based on the building size. It can be fixed on the bracing of the structure and assembled at the facade on every level of the building.

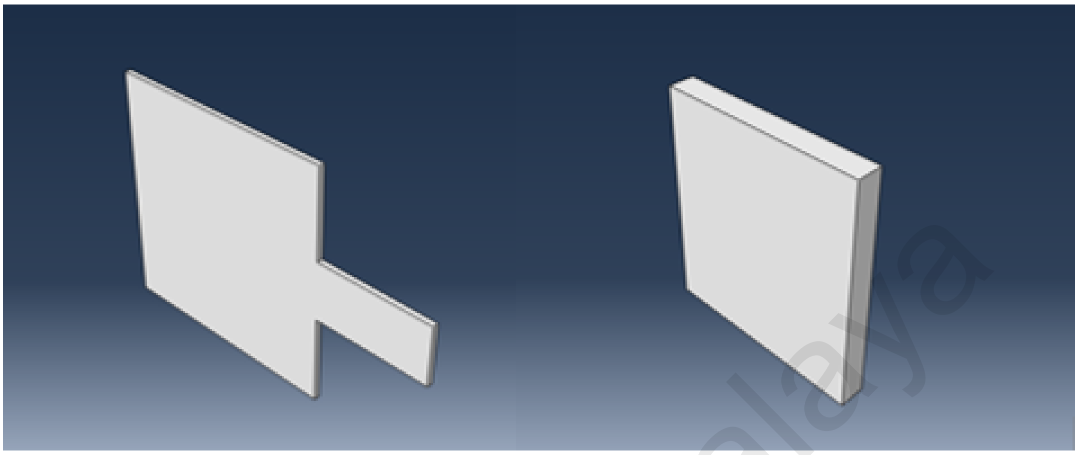

Fig. 4.24. Elements of sliding rubber damper.

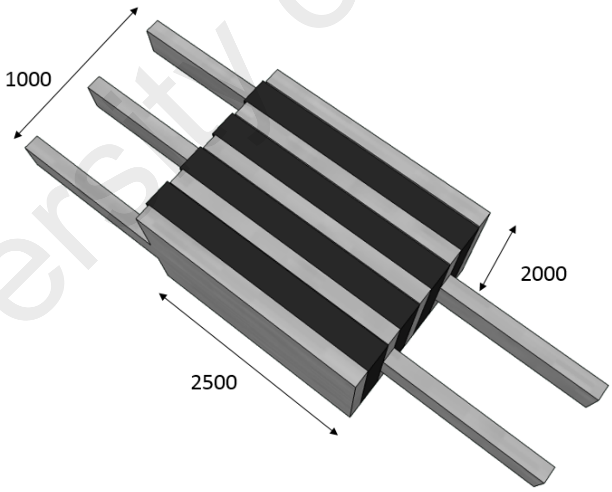

Fig. 4.25. Isotropic view of sliding rubber damper device (dimensions in mm).

4.3 Vibration test

Two modal testings were carried out, impact hammer test and shaker test. Impact hammer test was done to show the structure effect

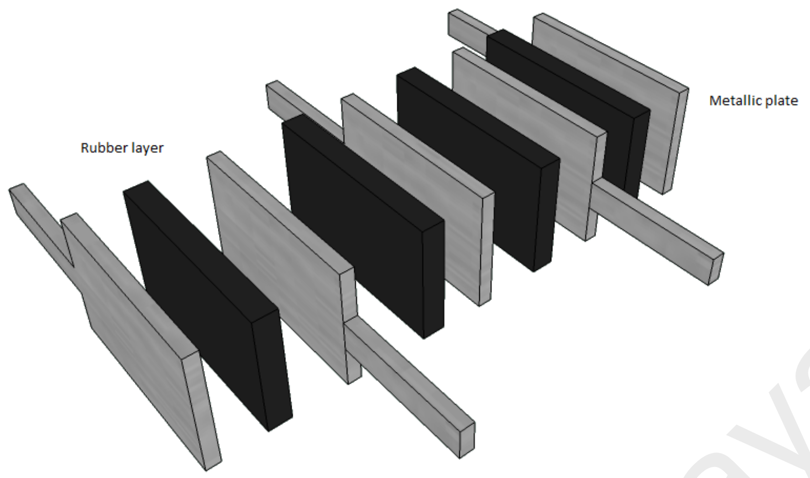

Fig. 4.26. Exploded view of sliding rubber damper device.

Fig. 4.27. Top view of sliding rubber damper device.

Fig. 4.28. Side view of sliding rubber damper device.

In the impact hammer modal test, the natural frequency of the structure during in-phase and out-of-phase is obtained, 21Hz and 33Hz respectively. First set of damping value of 10wt% carbon black and 25wt% carbon black SRD device is obtained from the calculation, which is 13.95 rad/s and 16.40 rad/s respectively. During the experiment, frequency response function, FRF is observed. Narrow and sharp peak is seen in 10wt% carbon black device whereas 25wt% carbon black device showed wider and broader peak. Sharp peak resulting lower damping while damping increases with lower peak in the waveform. Therefore SRD with 25wt% carbon black showed better performance in vibration isolation. Second test is carried out at the same natural frequency obtained from the first test. Shaker test is carried out at both the frequencies. The decay rate of the structure under specified frequency is plotted in the graph of log x against t. Effect of sliding rubber damper is more prominent for out-of-phase scenario where the damper is able to dampen the vibration exerted on the structure. Therefore the focus will be targeted in this case. The graphs of decay rate at 33Hz for two devices are shown in Figure 4.29 and Figure 4.30. Comparing 10wt% and 25wt% carbon black SRD device, the damping values are 20.963 rad/s and 24.65 rad/s respectively. This value indicates that SRD device with 25wt% carbon black has better damping performance than the previous device. It is able to absorb more vibration effect generated from the shaker.

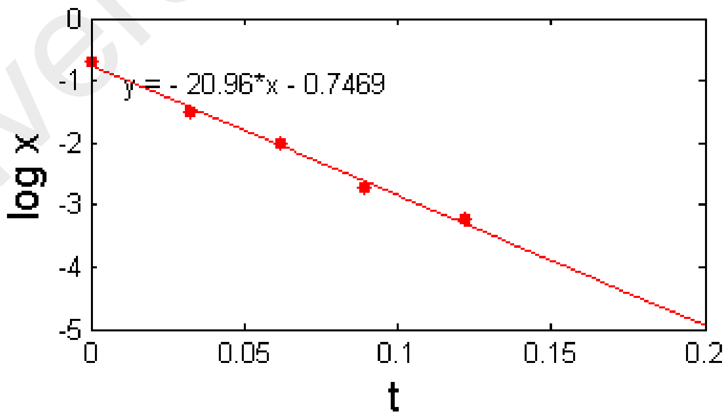

Fig. 4.29. Graph of log x against t for 10wt% carbon black specimens under shaker testing.

Referring to both the modal testing, two sets of damping values are obtained as shown in Table 4.1.

The difference of calculated damping value between two materials are 17%. Simi-

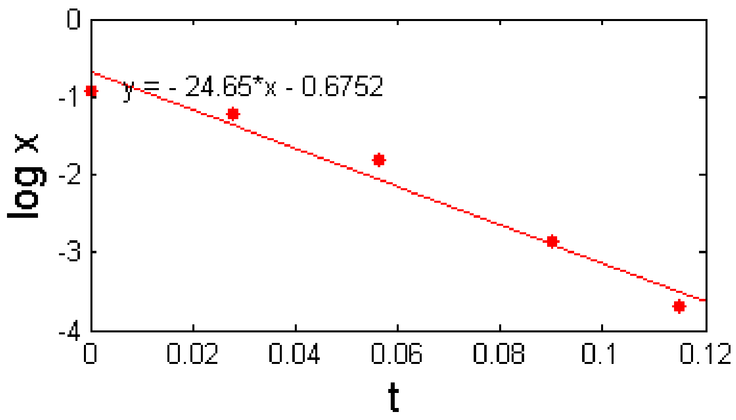

Fig. 4.30. Graph of log x against t for 25wt% carbon black specimens under shaker testing.

Fig. 4.1. Damping values from impact hammer modal testing (calculated) and shaker modal testing (experimental) of 10% and 25% carbon black SRD device

Device	Calculated damping value cal (rad/s)	Experimental damping value exp (rad/s)
10% carbon black	13.95	20.96
25% carbon black	16.40	24.65

larly, the difference between the experimental value is 17%. The first set of data generated from impact hammer modal testing is the average value calculated from the modal testing software. Damping value is directly obtained from the experimental results which showed more accurate reading compared to the calculated value.

CHAPTER 5: CONCLUSION AND FUTURE WORKS

5.1 Conclusion

To conclude the works, the objectives of this research as stated in Chapter 1 has been achieved.

Lifetime of elastomeric component in sliding rubber damper device is investigated. In this study, two rubber formulations with 10wt% and 25wt% carbon black natural rubber were used in the experimental work. Lifetime for both rubber formulations were presented in the form of Wöhler curves. It was shown that the fatigue life of natural rubber with 25wt% is longer than 10wt% when relevant prediction is used.

The lifetime of 10wt% and 25wt% carbon black were presented in the form of Wöhler curves with maximum principal stretch and strain energy density as the predictor. Rubber with higher carbon black content showed longer lifetime with the consideration of strain amplification factor.

Impact hammer modal testing and shaker testing were conducted to test the efficiency of the proposed device under vibration conditions. It is shown that device with 25wt% carbon black has better damping performance than 10wt% carbon black. It is able to absorb more vibration effect generated from the shaker.

A new earthquake energy dissipation device, sliding rubber damper (SRD) is proposed. Main component of SRD are rubber part and supporting material, metal plate. Utilizing the damping characteristics of rubber, SRD reduces vibrational damage of structure through shear. Experimental works has been conducted to validate the efficiency of the device. The device was awarded gold medal during the National Innovation and Invention Competition Through Exhibition 2015 (iCompEx'15).

5.2 Suggestions for future works

Based on the experimental results in Chapter 4, it is suggested that further investigation on different rubber formulation for rubber component in sliding rubber damper device is needed. From this suggested test, detailed multiaxial fatigue response of different rubber is compared thus aid in selecting better formulation which is suitable for earhquake vibration isolation application.

The simulation of sliding rubber damper in multiaxial loading using finite element code ABAQUS should be included as preliminary result for verifying the efficiency of the device in the future work.

REFERENCES

Abraham, F., Alshuth, T., & Jerrams, S. (2005). The effect of minimum stress and stress amplitude on the fatigue life of non strain crystallising elastomers. *Materials & design*, *26*(3), 239–245.

Abu-Abdeen, M. (2010). Single and double-step stress relaxation and constitutive modeling of viscoelasticbehavior of swelled and un-swelled natural rubber loaded with carbon black. *Mater. Design*, *31*(4), 2078-2084.

Andriyana, A., Saintier, N., & Verron, E. (2010). Configurational mechanics and critical plane approach: concept and application to fatigue failure analysis of rubberlike materials. *International journal of fatigue*, *32*(10), 1627–1638.

Auer, E., Doak, K., & Schaffner, I. (1958). Factors affecting laboratory cut-growth resistance of cold sbr tread stocks. *Rubber Chemistry and Technology*, *31*(1), 185–201.

Berton, G., Cruanes, C., Lacroix, F., Méo, S., & Ranganathan, N. (2015). Study of the fatigue behavior of the polychloroprene rubber with stress variation tests. *Procedia Engineering*, *101*, 413–420.

Beurrot-Borgarino, S., Huneau, B., Verron, E., & Rublon, P. (2013). Strain-induced crystallization of carbon black-filled natural rubber during fatigue measured by in situ synchrotron x-ray diffraction. *International Journal of fatigue*, *47*, 1–7.

Booth, E. D., & Key, D. (2006). *Earthquake design practice for buildings*. Thomas Telford.

Braden, M., & Gent, A. (1960). The attack of ozone on stretched rubber vulcanizates. i. the rate of cut growth. *Journal of Applied Polymer Science*, *3*(7), 90–99.

Bueche, F. (1960). Molecular basis for the mullins effect. *Journal of Applied Polymer Science*, *4*(10), 107–114.

Cadwell, S., Merrill, R., Sloman, C., & Yost, F. (1940). Dynamic fatigue life of rubber. *Industrial & Engineering Chemistry Analytical Edition*, *12*(1), 19–23.

Callister, W. D., & Rethwisch, D. G. (2012). *Fundamentals of materials science and engineering: an integrated approach*. John Wiley & Sons.

Candau, N., Chazeau, L., Chenal, J.-M., Gauthier, C., Ferreira, J., Munch, E., & Thiaudière, D. (2015). Strain induced crystallization and melting of natural rubber during dynamic cycles. *Physical Chemistry Chemical Physics*, *17*(23), 15331–15338.

Castaldo, P. (2014). *Integrated seismic design of structure and control systems*. Springer.

Chenal, J.-M., Gauthier, C., Chazeau, L., Guy, L., & Bomal, Y. (2007). Parameters governing strain induced crystallization in filled natural rubber. *Polymer*, *48*(23), 6893–6901.

Chou, H.-W., Huang, J.-S., & Lin, S.-T. (2007). Effects of thermal aging on fatigue of carbon black–reinforced epdm rubber. *Journal of applied polymer science*, *103*(2), 1244–1251.

Constantinou, M. C., Soong, T. T., & Dargush, G. F. (1998). *Passive energy dissipation systems for structural design and retrofit*. Multidisciplinary Center for Earthquake Engineering Research Buffalo, New York.

Diani, J., Fayolle, B., & Gilormini, P. (2009). A review on the mullins effect. *European Polymer Journal*, *45*(3), 601–612.

Dong, B., Liu, C., & Wu, Y.-P. (2014). Fracture and fatigue of silica/carbon black/natural rubber composites. *Polymer Testing*, *38*, 40–45.

Donnet, J. (2003). Nano and microcomposites of polymers elastomers and their reinforcement. *Composites Science and Technology*, *63*(8), 1085–1088.

Dorfmann, A., & Ogden, R. (2004). A constitutive model for the mullins effect with permanent set in particle-reinforced rubber. *International Journal of Solids and Structures*, *41*(7), 1855–1878.

Einstein, A. (1905). *Eine neue bestimmung der moleküldimensionen* (Unpublished doctoral dissertation). Buchdruckerei KJ Wyss.

El Fray, M., & Altstädt, V. (2003). Fatigue behaviour of multiblock thermoplastic elastomers. 1. stepwise increasing load testing of poly(aliphatic/aromatic-ester) copolymers. *Polymer*, *44*(16), 4643–4650.

Ghosh, P., Mukhopadhyay, R., & Stocek, R. (2016). Durability prediction of nr/br and nr/sbr blend tread compounds using tear fatigue analyser. *KGK-KAUTSCHUK GUMMI KUNSTSTOFFE*, *69*(6), 53–55.

Ghosh, P., Stocek, R., Gehde, M., Mukhopadhyay, R., & Krishnakumar, R. (2014). Investigation of fatigue crack growth characteristics of nr/br blend based tyre tread compounds. *International Journal of Fracture*, *188*(1), 9–21.

Green, A. E., & Adkins, J. E. (1960). *Large elastic deformations and non-linear continuum mechanics*. Clarendon Press.

Guth, E. (1945). Theory of filler reinforcement. *Journal of applied physics*, *16*(1), 20–25.

Guth, E., & Gold, O. (1938). On the hydrodynamical theory of the viscosity of suspensions. *Phys. Rev*, *53*(322), 2–15.

Guth, E., & Simha, R. (1936). Untersuchungen über die viskosität von suspensionen und lösungen. 3. über die viskosität von kugelsuspensionen. *Colloid & Polymer Science*, *74*(3), 266–275.

Harbour, R. J., Fatemi, A., & Mars, W. V. (2008). Fatigue crack orientation in nr and sbr under variable amplitude and multiaxial loading conditions. *Journal of Materials Science*, *43*(6), 1783–1794.

Herzig, A., Johlitz, M., & Lion, A. (2015). An experimental set-up to analyse the oxygen consumption of elastomers during ageing by using a differential oxygen analyser. *Continuum Mechanics and Thermodynamics*, *27*(6), 1009.

Hon, A., Busfield, J., & Thomas, A. (2003). Filler reinforcement in rubber carbon black systems. *CONSTITUTIVE MODELS FOR RUBBER*, 301–308.

Huneau, B., Masquelier, I., Marco, Y., Le Saux, V., Noizet, S., Schiel, C., & Charrier, P. (2016). Fatigue crack initiation in a carbon black–filled natural rubber. *Rubber Chemistry and Technology*, *89*(1), 126–141.

Iizuka, M. (2000). A macroscopic model for predicting large-deformation behaviors of laminated rubber bearings. *Engineering Structures*, *22*(4), 323–334.

Irvine, T. (2000). an introduction to frequency response functions. *Rapport, College of Engineering and Computer Science*.

Irwin, P. A., & Breukelman, B. (2001). Recent applications of damping systems for wind response. In *Proceedings of the sixth world congress of the council on tall buildings and urban habitat, melbourne, australia, february.*

Ismail, H., Muniandy, K., & Othman, N. (2012). Fatigue life, morphological studies, and thermal aging of rattan powder-filled natural rubber composites as a function of filler loading and a silane coupling agent. *BioResources*, *7*(1), 0841–0858.

Johlitz, M., & Lion, A. (2013). Chemo-thermomechanical ageing of elastomers based on multiphase continuum mechanics. *Continuum Mechanics and Thermodynamics*, 1–20.

Kar, K. K., & Bhowmick, A. K. (1997). High-strain hysteresis of rubber vulcanizates over a range of compositions, rates, and temperatures. *Journal of applied polymer science*, *65*(7), 1429–1439.

Kelly, J. M., & Konstantinidis, D. (2011). *Mechanics of rubber bearings for seismic and vibration isolation*. John Wiley & Sons.

Kind, D. J., & Hull, T. R. (2012). A review of candidate fire retardants for polyisoprene. *Polymer Degradation and Stability*, *97*(3), 201–213.

Klüppel, M. (2009). The role of filler networking in fatigue crack propagation of elastomers under high-severity conditions. *Macromolecular Materials and Engineering*, *294*(2), 130–140.

Kraus, G. (1978). Reinforcement of elastomers by carbon black. *Rubber chemistry and Technology*, *51*(2), 297–321.

Lake, G. (1995). Fatigue and fracture of elastomers. *Rubber Chemistry and Technology*, *68*(3), 435–460.

Lake, G., & Lindley, P. (1964). Cut growth and fatigue of rubbers. ii. experiments on a noncrystallizing rubber. *Journal of Applied Polymer Science*, *8*(2), 707–721.

Lake, G., & Lindley, P. (1966). Fatigue of rubber at low strains. *Journal of Applied Polymer Science*, *10*(2), 343–351.

Le Cam, J.-B., Huneau, B., & Verron, E. (2008). Description of fatigue damage in carbon black filled natural rubber. *Fatigue & Fracture of Engineering Materials & Structures*, *31*(12), 1031–1038.

Le Cam, J.-B., Huneau, B., & Verron, E. (2013). Fatigue damage in carbon black filled natural rubber under uni-and multiaxial loading conditions. *International Journal of Fatigue*, *52*, 82–94.

Lectez, A.-S., Verron, E., Huneau, B., Beranger, A., & Le Brazidec, F. (2013). Characterization of elastomers under simultaneous tension and torsion for application to engine mounts. In *Proceedings of the 8th european conference on constitutive models for rubber (eccmr)* (Vol. 8, pp. 585–590).

Le Gac, P.-Y., Arhant, M., Davies, P., & Muhr, A. (2015). Fatigue behavior of natural rubber in marine environment: Comparison between air and sea water. *Materials & Design (1980-2015)*, *65*, 462–467.

Legorju-Jago, K., & Bathias, C. (2002). Fatigue initiation and propagation in natural and synthetic rubbers. *International Journal of Fatigue*, *24*(2), 85–92.

Lewangamage, C. S., Abe, M., Fujino, Y., & Yoshida, J. (2004). Design criteria for seismic isolation rubber bearings. In *13 wcee: 13 th world conference on earthquake engineering conference proceedings.*

Lion, A. (1996). A constitutive model for carbon black filled rubber: experimental investigations and mathematical representation. *Continuum Mechanics and Thermodynamics*, *8*(3), 153–169.

Lion, A., & Johlitz, M. (2012). On the representation of chemical ageing of rubber in continuum mechanics. *International Journal of Solids and Structures*, *49*(10), 1227–1240.

Loo, M., Le Cam, J.-B., Andriyana, A., Robin, E., & Coulon, J. (2016). Effect of swelling on fatigue life of elastomers. *Polymer Degradation and Stability*, *124*, 15–25.

Loo, M. S., Le Cam, J.-B., Andriyana, A., Robin, E., & Afifi, A. M. (2015). Fatigue of swollen elastomers. *International Journal of Fatigue*, *74*, 132–141.

Luksameevanish, V., Seadan, M., Kopoonpat, S., et al. (2006). Shape factor and carbon black loading effect on fea prediction of bearing behaviour. *Journal of Rubber Research*, *9*(3), 159–177.

Lyon, R. E., Speitel, L., Walters, R. N., & Crowley, S. (2003). Fire-resistant elastomers. *Fire and materials*, *27*(4), 195–208.

Mannan, S. (2013). *Lees' process safety essentials: Hazard identification, assessment and control*. Butterworth-Heinemann.

Marco, Y., Le Saux, V., Calloch, S., & Charrier, P. (2010). X-ray computed μ-tomography: a tool for the characterization of fatigue defect population in a polychloroprene rubber. *Procedia Engineering*, *2*(1), 2131–2140.

Mark, J. E., Erman, B., & Roland, M. (2013). *The science and technology of rubber*. Academic press.

Mars, W., & Fatemi, A. (2002). A literature survey on fatigue analysis approaches for rubber. *International Journal of Fatigue*, *24*(9), 949–961.

Mars, W., & Fatemi, A. (2004a). Fatigue crack nucleation and growth in filled natural rubber subjected to multiaxial stress states. In *Seventh international conference on biaxial/multiaxial fatigue and fracture, berlin* (pp. 329–334).

Mars, W., & Fatemi, A. (2004b). A novel specimen for investigating the mechanical behavior of elastomers under multiaxial loading conditions. *Experimental mechanics*, *44*(2), 136–146.

Mars, W., & Fatemi, A. (2006). Multiaxial stress effects on fatigue behavior of filled natural rubber. *International Journal of Fatigue*, *28*(5), 521–529.

Martinez, J. S., Toussaint, E., Balandraud, X., Le Cam, J.-B., & Berghezan, D. (2015). Heat and strain measurements at the crack tip of filled rubber under cyclic loadings using full-field techniques. *Mechanics of Materials*, *81*, 62–71.

Matsagar, V. A., & Jangid, R. S. (2005). Viscoelastic damper connected to adjacent structures involving seismic isolation. *Journal of civil engineering and management*, *11*(4), 309–322.

Merckel, Y. (2012). *Experimental characterization and modeling of the mechanical behavior of filled rubbers under cyclic loading conditions* (Unpublished doctoral dissertation). Ecole Centrale de Lille.

Mohammed, A., Nemat-Alla, M. M., & Emara, K. M. (2014). Influence of cyclic loading on fatigue behaviour of sbr and nbr compounds with different contents of carbon black.

Moreschi, L. M. (2000). *Seismic design of energy dissipation systems for optimal structural performance* (Unpublished doctoral dissertation). Virginia Polytechnic Institute and State University.

Mostafa, A., Abouel-Kasem, A., Bayoumi, M., & El-Sebaie, M. (2009). Effect of carbon black loading on the swelling and compression set behavior of sbr and nbr rubber compounds. *Materials & Design*, *30*(5), 1561–1568.

Mullins, L. (1950). Thixotropic behavior of carbon black in rubber. *Rubber Chemistry and Technology*, *23*(4), 733–743.

Murty, C., Goswami, R., Vijayanarayanan, A., & Mehta, V. V. (2012). Earthquake behaviour of buildings.

Nakason, C., Wannavilai, P., & Kaesaman, A. (2006). Effect of vulcanization system on properties of thermoplastic vulcanizates based on epoxidized natural rubber/polypropylene blends. *Polymer testing*, *25*(1), 34–41.

Neuhaus, C., Lion, A., Johlitz, M., Heuler, P., Barkhoff, M., & Duisen, F. (2017). Fatigue behaviour of an elastomer under consideration of ageing effects. *International Journal of Fatigue*, *104*, 72–80.

Ngolemasango, F. E., Bennett, M., & Clarke, J. (2008). Degradation and life prediction of a natural rubber engine mount compound. *Journal of applied polymer science*, *110*(1), 348–355.

Nielsen, L. E. (1966). Simple theory of stress-strain properties of filled polymers. *Journal of Applied Polymer Science*, *10*(1), 97–103.

Omnès, B., Thuillier, S., Pilvin, P., Grohens, Y., & Gillet, S. (2008). Effective properties of carbon black filled natural rubber: experiments and modeling. *Composites Part A: Applied Science and Manufacturing*, *39*(7), 1141–1149.

Poisson, J.-L., Lacroix, F., Meo, S., Berton, G., & Ranganathan, N. (2011). Biaxial fatigue behavior of a polychloroprene rubber. *International Journal of Fatigue*, *33*(8), 1151–1157.

Qi, H., & Boyce, M. (2004). Constitutive model for stretch-induced softening of the stress–stretch behavior of elastomeric materials. *Journal of the Mechanics and Physics of Solids*, *52*(10), 2187–2205.

Rai, N. K., Reddy, G., Ramanujam, S., Venkatraj, V., & Agrawal, P. (2009). Seismic response control systems for structures. *Defence Science Journal*, *59*(3), 239–251.

Rey, T., Chagnon, G., Le Cam, J.-B., & Favier, D. (2013). Influence of the temperature on the mechanical behaviour of filled and unfilled silicone rubbers. *Polymer Testing*, *32*(3), 492–501.

Roberts, B., & Benzies, J. (1977). The relationship between uniaxial and equibiaxial fatigue in gum and carbon black filled vulcanizates. *Proceedings of rubbercon*, *77*(2.1), 2–1.

Rublon, P., Huneau, B., Verron, E., Saintier, N., Beurrot, S., Leygue, A., … Berghezan, D. (2014). Multiaxial deformation and strain-induced crystallization around a fatigue crack in natural rubber. *Engineering Fracture Mechanics*, *123*, 59–69.

Sae-Oui, P., Sirisinha, C., & Hatthapanit, K. (2007). Effect of blend ratio on aging, oil and ozone resistance of silica-filled chloroprene rubber/natural rubber (cr/nr) blends. *Express Polymer Letters*, *1*(1), 8–14.

Sahakaro, K., Talma, A. G., Datta, R. N., & Noordermeer, J. W. (2007). Blending of nr/br/epdm by reactive processing for tire sidewall applications. ii. characterization. *Journal of applied polymer science*, *103*(4), 2547–2554.

Saintier, N., Cailletaud, G., & Piques, R. (2006a). Crack initiation and propagation under multiaxial fatigue in a natural rubber. *Int. J. Fatigue*, *28*(1), 61–72.

Saintier, N., Cailletaud, G., & Piques, R. (2006b). Multiaxial fatigue life prediction for a natural rubber. *Int. J. Fatigue*, *28*(5), 530–539.

Saintier, N., Cailletaud, G., & Piques, R. (2011). Cyclic loadings and crystallization of natural rubber: An explanation of fatigue crack propagation reinforcement under a positive loading ratio. *Materials Science and Engineering: A*, *528*(3), 1078–1086.

Santangelo, P., & Roland, C. (1995). Failure properties of natural rubber double networks. *Rubber Chemistry and Technology*, *68*(1), 124–131.

Shrimali, M., Bharti, S., & Dumne, S. (2015). Seismic response analysis of coupled building involving mr damper and elastomeric base isolation. *Ain Shams Engineering Journal*.

Sirisinha, C., & Prayoonchatphan, N. (2001). Study of carbon black distribution in br/nbr blends based on damping properties: influences of carbon black particle size, filler, and rubber polarity. *Journal of applied polymer science*, *81*(13), 3198–3203.

Smallwood, H. M. (1944). Limiting law of the reinforcement of rubber. *Journal of applied physics*, *15*(11), 758–766.

Soong, T., & Spencer, B. (2000). Active, semi-active and hybrid control of structures. *Bulletin of the New Zealand National Society for Earthquake Engineering*, *33*(3), 387–402.

Soong, T., & Spencer, B. (2002). Supplemental energy dissipation: state-of-the-art and state-of-the-practice. *Engineering Structures*, *24*(3), 243–259.

Srinivas, H., & Nakagawa, Y. (2008). Environmental implications for disaster preparedness: lessons learnt from the indian ocean tsunami. *Journal of Environmental Management*, *89*(1), 4–13.

Stadlbauer, F., Koch, T., Archodoulaki, V.-M., Planitzer, F., Fidi, W., & Holzner, A. (2013). Influence of experimental parameters on fatigue crack growth and heat build-up in rubber. *Materials*, *6*(12), 5502–5516.

Stevenson, A. (1983). A fracture mechanics study of the fatigue of rubber in compression. *International journal of fracture*, *23*(1), 47–59.

Suryatal, B., Phakatkar, H., Rajkumar, K., Thavamani, P., et al. (2015). Fatigue life estimation of an elastomeric pad by ε-n curve and fea. *Journal of Surface Engineered Materials and Advanced Technology*, *5*(02), 85.

Symans, M., Charney, F., Whittaker, A., Constantinou, M., Kircher, C., Johnson, M., & McNamara, R. (2008). Energy dissipation systems for seismic applications: current practice and recent developments. *Journal of Structural Engineering*, *134*(1), 3–21.

Toki, S., Fujimaki, T., & Okuyama, M. (2000). Strain-induced crystallization of natural rubber as detected real-time by wide-angle x-ray diffraction technique. *Polymer*, *41*(14), 5423–5429.

Topkaya, C., Yura, J. A., & Williamson, E. B. (2004). Composite shear stud strength at early concrete ages. *Journal of Structural Engineering*, *130*(6), 952–960.

Treloar, L. (2005). *The physics of rubber elasticity*. Oxford University Press, USA.

Trethewey, M., & Cafeo, J. (1992). Tutorial: signal processing aspects of structural impact testing. *The International Journal of Analytical and Experimental Modal Analysis*, *7*(2), 129–149.

Ulu, K. N., Huneau, B., Le Gac, P.-Y., & Verron, E. (2016). Fatigue resistance of natural rubber in seawater with comparison to air. *International Journal of Fatigue*, *88*, 247–256.

Vinod, V., Varghese, S., & Kuriakose, B. (2002). Degradation behaviour of natural rubber–aluminium powder composites: effect of heat, ozone and high energy radiation. *Polymer Degradation and Stability*, *75*(3), 405–412.

Voet, A. (1980). Reinforcement of elastomers by fillers: Review of period 1967–1976. *Journal of Polymer Science: macromolecular reviews*, *15*(1), 327–373.

Xie, Z., Miao, C., Wan, Z., & Wei, Y. (2005). Investigation of the carbon-black network in natural rubber under cyclic deformation. *Journal of Macromolecular Science, Part B: Physics*, *44*(3), 345–351.

Yamaguchi, K., Busfield, J., & Thomas, A. (2003). Electrical and mechanical behavior of filled elastomers. i. the effect of strain. *Journal of Polymer Science Part B: Polymer Physics*, *41*(17), 2079–2089.

Zarrin-Ghalami, T., & Fatemi, A. (2013). Multiaxial fatigue and life prediction of elastomeric components. *International Journal of Fatigue*, *55*, 92–101.

Zhou, Y., Jerrams, S., & Chen, L. (2013). Multi-axial fatigue in magnetorheological elastomers using bubble inflation. *Materials & Design*, *50*, 68–71.

LIST OF AWARDS AND PUBLICATIONS

AWARDS

1. National Innovation and Invention Competition Through Exhibition 2015 (iCompEx'15). 24-26 March 2015. Politeknik Sultan Abdul Halim Mu'adzam Shah, Kedah, Malaysia. (Gold Medal)

JOURNAL PUBLICATIONS

1. **Tee, Y. L.**, Loo, M.S. & Andriyana, A. (2018). Recent advances on fatigue of rubber after the literature survey by Mars and Fatemi in 2002 and 2004. *International Journal of Fatigue*. Article in Press. (ISI Q1)

2. Ch'ng, S. Y., Andriyana, A., **Tee, Y. L.**, & Verron, E. (2015). Effects of carbon black and the presence of static mechanical strain on the swelling of elastomers in solvent. *Materials*, 8(3), 884-898. (ISI Q1)

3. Ch'ng, S. Y., Andriyana, A., **Tee, Y. L.**, & Verron, E. (2014). Effect of carbon black content on the swelling of elastomers in solvent in the presence of static mechanical loading. *Materials Research Innovations*, 18(sup6), S6-314-S6-317. (ISI Q4)

4. **Tee, Y. L.**, Andriyana, A., Huneau, B., Verron, E., Suhatril, M. & Ong, Z.C. (2017). Fatigue characteristics and modal analysis of filled natural rubber for earthquake energy dissipation application. *Plos One*. (Under review)

5. **Tee, Y. L.**, Loo, M.S., Andriyana, A. & Suhatril, M. (2018). Construction of Wohler curve of rubber with reference of carbon black content. (In progress)

CONFERENCE PUBLICATIONS

1. **Tee, Y. L.**, Suhatril, M., Andriyana, A. & Khatibi, H. (2015). Sliding rubber damper as earthquake energy dissipation device on structural buildings. *9th Asean Postgraduate Seminar (APGS)*. 8 December 2015. Kuala Lumpur, Malaysia.

2. Ch'ng, S. Y., Andriyana, A., **Tee, Y. L.**, & Verron, E. (2014). Effect of carbpn black content on the swelling of elastomers in solvent in the presence of static mechanical loading. *International Conference on the Science and Engineering of Materials.* 13-14 November 2013. Kuala Lumpur, Malaysia.